

U. S. GEOLOGICAL SURVEY
SAUDI ARABIAN PROJECT REPORT 278

GEOPHYSICAL INVESTIGATIONS
OF THE KUTAM ANCIENT MINE AND VICINITY,
KINGDOM OF SAUDI ARABIA

by

H. Richard Blank, Vincent J. Flanigan, Mark E. Gettings,
and Habib M. Merghelani

This report is preliminary and has not been reviewed for conformity with Geological Survey editorial standards. Use of trade names is for descriptive purposes only and does not constitute endorsement by the U.S. Geological Survey.

U.S. Geological Survey
Open-File Report 80-1268

U.S. Geological Survey
Jiddah, Saudi Arabia

1980

The work on which this report is based was performed in accordance with a cooperative agreement between the U. S. Geological Survey and the Ministry of Petroleum and Mineral Resources, Kingdom of Saudi Arabia.

This report is preliminary and has not been edited or reviewed for conformity with U. S. Geological Survey standards and nomenclature.

CONTENTS

	<u>Page</u>
ABSTRACT.....	1
INTRODUCTION.....	2
HISTORY OF EXPLORATION.....	4
GEOLOGY AND MINERALIZATION.....	6
ELECTRIC LOGS.....	8
RADIOMETRIC SURVEY.....	11
SELF-POTENTIAL SURVEYS.....	12
TURAM ELECTROMAGNETIC SURVEYS.....	14
INDUCED POLARIZATION SURVEYS.....	25
Dipole-dipole.....	27
Mise-a-la-masse.....	31
INPUT AIRBORNE ELECTROMAGNETIC SURVEY.....	37
MAGNETIC SURVEY.....	38
SUMMARY AND CONCLUSIONS.....	40
REFERENCES CITED.....	45
APPENDIX.....	47

ILLUSTRATIONS

[Plates are in pocket]

- | | | | |
|----------|---|---|----------------|
| Plate 1. | Topographic map of Kutam mine showing grids used in geochemical and geophysical surveys | } | <i>sheet 1</i> |
| 2. | Topographic and geochemical map of the Kutam mine showing sample locations anomalous in copper and zinc | | |
| 3. | Geologic map of the Kutam mine | } | <i>sheet 2</i> |
| 4. | Vertical sections through diamond drill holes, Kutam mine | | |
| 5. | Schematic representations of ore reserve blocks, Kutam mine | } | <i>sheet 3</i> |
| 6. | Self-potential and resistivity logs of drill holes KA-1, KA-2, KA-3, and KA-4, Kutam mine | | |
| 7. | Gamma-radiation map, Kutam mine (potassium channel) | } | <i>sheet 2</i> |
| 8. | Self-potential map, Kutam mine | | |
| 9. | Turam electromagnetic survey, Kutam mine: Amplitude ratio map (660 Hz) | } | <i>sheet 4</i> |
| 10. | Turam electromagnetic survey, Kutam mine: Phase difference map (660 Hz) | | |
| 11. | Turam electromagnetic survey, Kutam mine: Amplitude ratio map (220 Hz) | | |
| 12. | Turam electromagnetic survey, Kutam mine: Phase difference map (220 Hz) | | |
| 13. | Induced polarization dipole-dipole survey, Kutam mine: Pseudosections of frequency effect | | |

- Plate 14. Induced polarization dipole-dipole survey, Kutam mine: Pseudosections of apparent resistivity
- 15. Induced polarization dipole-dipole survey, Kutam mine: Pseudosections of apparent metal factor
- 16. Induced polarization mise-a-la-masse survey, Kutam mine: Maps of frequency effect for source electrode in drill holes KA-1 and KA-2
- 17. Induced polarization mise-a-la-masse survey, Kutam mine: Map of frequency effect for source electrode in drill hole KA-3
- 18. Induced polarization mise-a-la-masse survey, Kutam mine: Maps of apparent resistivity for source electrode in drill holes KA-1 and KA-2
- 19. Induced polarization mise-a-la-masse survey, Kutam mine: Map of apparent resistivity for source electrode in drill hole KA-3
- 20. Induced polarization mise-a-la-masse survey, Kutam mine: Maps of apparent metal factor for source electrode in drill holes KA-1 and KA-2
- 21. Induced polarization mise-a-la-masse survey, Kutam mine: Map of apparent metal factor for source electrode in drill hole KA-3
- 22. INPUT survey, Kutam test area: Electromagnetic map
- 23. INPUT survey, Kutam test area: Isomagnetic contour map
- 24. Magnetic total-field intensity anomaly map, Kutam mine
- 25. Map of principal radiometric and electrical anomalies, Kutam mine
- 26. Geophysical trend map, Kutam mine

sheet 5

sheet 6

sheet 7

sheet 8

Page

Figure 1.	Index map of western Saudi Arabia showing location of the Kutam ancient mine.....	3
2.	Comparison of self-potential logs of drill holes KA-1, KA-2, KA-3, and KA-4, Kutam mine.	10
3.	Turam profiles, line 200N (660 Hz).....	18
4.	Turam profiles, line 18S (660 Hz).....	20
5.	Turam profiles, line 18S (220 Hz).....	21
6.	Turam profiles, line 240S (660 Hz).....	24
7.	Diagram showing method of construction of dipole-dipole pseudosections.....	28

GEOPHYSICAL INVESTIGATIONS
OF THE KUTAM ANCIENT MINE AND VICINITY,
KINGDOM OF SAUDI ARABIA

by

H. Richard Blank, Vincent J. Flanigan, Mark E. Gettings,
and Habib M. Merghelani

ABSTRACT

A program of ground geophysical investigations was carried out during 1974 and 1975 in support of mineral exploration in the vicinity of the Kutam ancient mine, a massive sulfide deposit associated with a northwest-trending shear zone of late Precambrian age in southwestern Saudi Arabia. The work included radiometric, self-potential (SP), Turam electromagnetic (EM), induced polarization (dipole-dipole and mise-a-la-masse), and ground magnetic surveys, in addition to single-point resistivity and self-potential logs of four drill holes that penetrated mineralization. In 1977 the area was also covered by an INPUT airborne electromagnetic survey.

The drilled ore deposit is associated with a negative SP anomaly of more than 300 mv and with an induced polarization (IP) anomaly of 5-10 percent frequency effect. There is some suggestion of potassium enrichment, probably related to a pre-mineralization stage of hydrothermal alteration.

Only very weak Turam responses are found over the ore, but instead, a sharp linear Turam anomaly is disposed adjacent to the deposit on either side in the principal shear zone. Neither Turam source produces a polarization anomaly. The northwest EM, central IP/SP, and southeast EM anomalies form an en echelon triad tentatively interpreted as the expression of structures produced by right-lateral shear.

The Turam anomalies occur in low-lying, weakly pyritized areas and are inferred to result from ionic conduction, whereas the upper part of the ore deposit is drier (because it forms a ridge), contains less pyrite, and is in part silicified, all of which may have inhibited the electromagnetic response. It seems likely that the Turam survey did not achieve satisfactory coupling with the ore body, although because of its steeply plunging, rod-like habit the ore is less than an ideal target. Nevertheless the INPUT survey identified a conductivity anomaly favorable for prospecting.

The principal area of alteration and mineralization is revealed on the ground magnetic map as a "quiet" zone of subdued magnetic contrasts as a consequence of leaching of magnetite.

A belt of strong east-west geophysical-anomaly trends intersects the Kutam shear zone at the southeastern termination of the drilled ore deposit. Its significance is not clear, but IP and other geophysical survey data suggests the possibility that a blind mineralized zone is present to the southwest of the ancient workings. Turam and IP data also suggest an exploration target to the north of the workings beneath Wajid sandstone. On the other hand, the only known mineralization occurs in the Kutam shear zone, and this structure probably offers the best chance for extending the resources of the mine. Any ore lying at considerable depth beneath the Turam current concentrations would very likely have escaped detection.

INTRODUCTION

The Kutam ancient mine is located at lat 17°35'55" N., long 43°34'10" E., in the southwestern part of the Mayza 30-minute quadrangle, about 115 km southeast of Khamis Mushayt and a few kilometers north of the Yemen border (fig. 1). It can be reached by following 3 km of unimproved track leading east from the Khamis Mushayt-Najran paved highway. The terrain in this part of the Asir is a dissected upland of several hundred meters relief characterized by buttes and mesas of Paleozoic Wajid Sandstone that overlies crystalline metamorphic rocks of the Precambrian basement. Vegetation is sparse but thunderstorms generated over the nearby Hijaz-Asir escarpment occur occasionally, particularly in the winter months. In the vicinity of the mine, malachite shows and numerous pits, shafts, waste-mantled slopes, and slag heaps all bear witness to the existence of a large-scale base metal mining operation in the distant past.

The mine was "rediscovered" by R. E. Anderson in 1973 during the course of geologic mapping of the Mayza quadrangle (Anderson, 1978). Subsequent geologic and geochemical investigations by Anderson, M. R. Dehlavi, W. P. Puffet, A. M. Helaby, and C. W. Smith, supported by geophysical work and by a diamond drilling program consisting of eight holes aggregating 1929 m in length, have confirmed the presence of a moderate-size copper-zinc sulfide ore body beneath the ancient workings. The geology and ore deposits of the mine area are described in a separate report

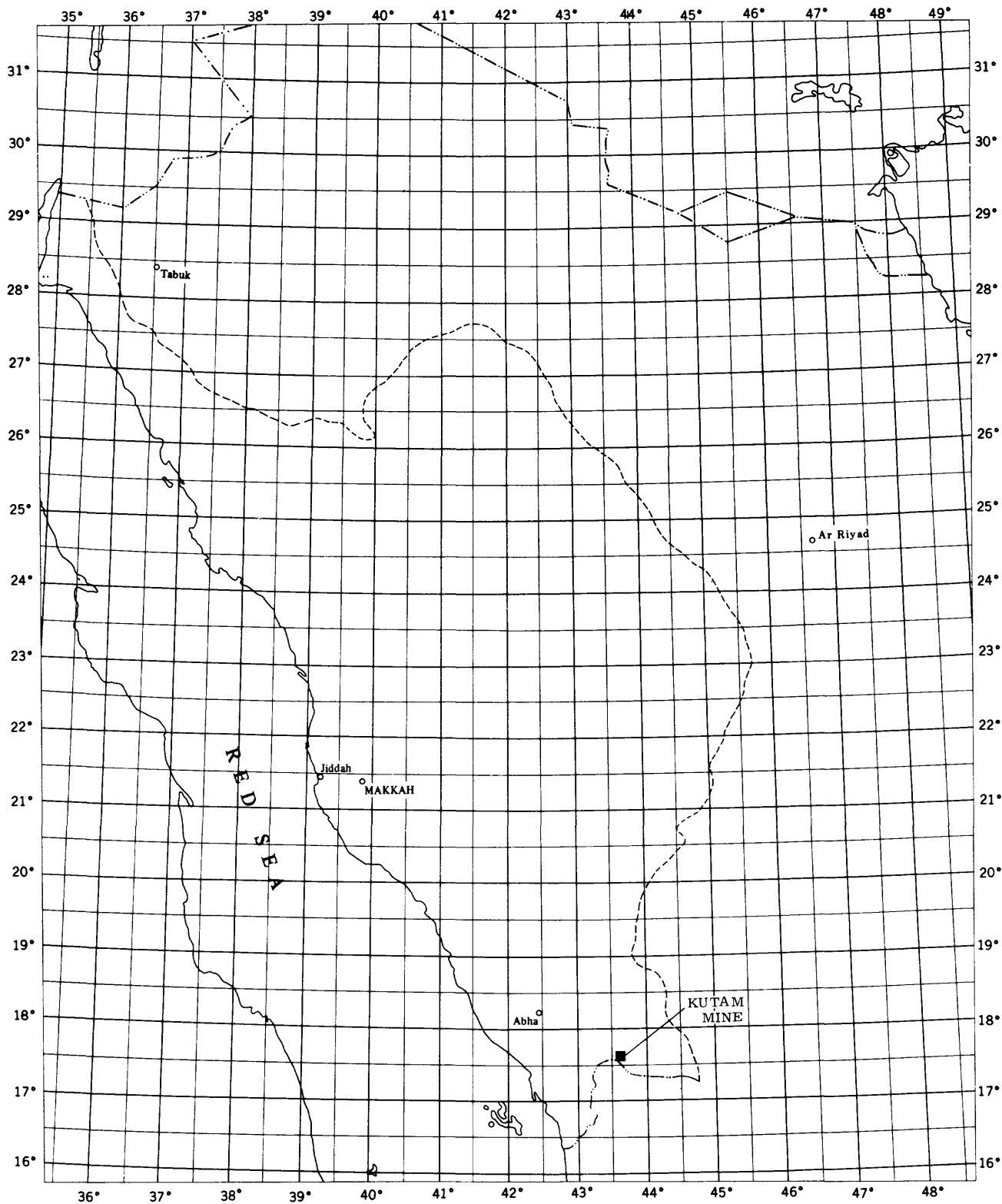


Figure 1.—Index map of western Saudi Arabia showing location of the Kutam ancient mine.

by Smith and others (1970). Their results are also summarized in a section of the present report and several of their illustrations are reproduced here for convenience in relating geophysical data to geology. Although enough geologic data are included in the geophysical report to enable it to stand alone, the reader should consult the full geologic report before undertaking any serious evaluation of the geophysical findings.

The ground geophysical surveys at Kutam that are discussed here were carried out by the staff of the combined U.S. Geological Survey/Directorate General of Mineral Resources Geophysics Section in 1974 and 1975 as part of the overall economic mineral evaluation program of the USGS Mission, in accordance with its Work Agreement with the Ministry of Petroleum and Mineral Resources.

HISTORY OF EXPLORATION

Detailed geological and geochemical investigations of the Kutam mine area were initiated by R. E. Anderson and M. R. Dehlavi in October 1973. Geophysical field work was begun in February 1974 by Flanigan and Merghelani. Self-potential (SP), Turam electromagnetic (EM), and gamma-radiation measurements were made by the geophysical survey team at 20-m or 40-m intervals along traverses spaced 40 m apart and trending N.60°E., normal to the mean geologic strike of N.30°W., in the vicinity of the ancient workings. A plane-table topographic map of the prospect area at scale 1:2,000 and contour interval 2 m, and a grid oriented east-west with marked cairns at 40-m intervals were made during this period by K. S. McLean and M. B. Almutayri. The map and the grid were later extended to the southeast by C. W. Smith. These grid points were used in the geochemical sampling program and for all subsequent geophysical surveys, even though traverses were not oriented in the direction most suitable for geophysical measurements.

The topographic base map for the prospect area is given on plate 1. In addition, this map shows the N.60°E. survey net, the east-west grid, the locations of diamond drill holes and ancient mine workings, and the principal geodetic points for the topographic survey.

Results of the geochemical survey are presented on plate 2. This map shows a concentration of copper anomalies in the immediate vicinity of the ancient workings, and somewhat more extensively distributed zinc anomalies to the northwest and southeast of the mine.

Preliminary geologic mapping and results of geochemical and geophysical surveys were considered favorable enough to warrant exploratory drilling. A program of diamond drilling by the Arabian Drilling Company (ADC) was commenced in mid-1974 and continued through the first half of 1975. Additional geologic mapping and geochemical sampling aimed at finding possible extensions of the ore body along strike were carried out by C. W. Smith during this period of drilling. Additional geophysical work consisting of induced polarization (IP) and ground magnetic surveys, as well as extensions of the previous self-potential and Turam electromagnetic surveys, were made by Blank, Merghelani, and Gettings, assisted by A. Showail and A. Uthman. Also, electric logs (self-potential and single-point resistivity) were made in drill holes KA-1, KA-2, KA-3, and KA-4. Although the diamond drilling program and much geophysical field work were carried out at about the same time, selection of nearly all the drill sites was influenced to some extent by geophysical data.

Following completion of the USGS work, an exploration concession was acquired by Noranda Exploration Ltd. for a very large area that included the Kutam mine. Noranda geophysicists carried out pulsed electromagnetic (PEM) and ground magnetic surveys of the mine area in September 1976, and drill hole and mise-a-la-masse induced potential surveys in February and March 1977. A program of additional diamond drilling and geologic mapping was conducted concurrently. This exploration concession was subsequently relinquished.

In March 1977 the Arabian Geophysical and Surveying Company (ARGAS), through its affiliate, Geoterrex Ltd. of Canada, flew 12 test lines across the Kutam ore deposit and vicinity with a Barringer Mark V "INPUT" pulsed electromagnetic system. This work was part of a larger program of INPUT surveys carried out under USGS supervision on behalf of the Ministry of Petroleum and Mineral Resources by means of a contract with Watts, Griffis, and McQuat, Ltd. (Anonymous, 1978; Wynn and Blank, 1979).

The availability of so many different types of geophysical data for an ore deposit that has been extensively mapped and drilled makes Kutam an excellent candidate for an exploration case history. It is hoped that some of the results presented here can find application in exploration for base metal deposits elsewhere on the Arabian Shield.

GEOLOGY AND MINERALIZATION

The geologic map of the mine area by Smith and others (1978) is shown on plate 3. The principal host rock of the ore zone, and indeed the prevalent rock type in the vicinity, is quartz porphyry. It is associated with stratified metavolcanic rocks of intermediate to mafic composition, but no general agreement exists as to whether the quartz porphyry is intrusive, part of the metavolcanic sequence, or both. Minor beds of graphitic schist, marble, and jasperoid are also present. All of these rock units are metamorphosed to amphibolite facies and within the ore zone are intensely sheared, recrystallized, and hydrothermally altered. Rocks of the ore zone include chlorite-quartz schist, chlorite-sericite-quartz schist, sericite-quartz schist, chlorite schist, talc schist, and massive quartz. The chlorite-bearing rocks are commonly garnetiferous. Dikes of mafic composition, generally with northerly strikes but discontinuously exposed, are believed to be the youngest rocks present and are only weakly or not at all mineralized.

A pervasive foliation imparted by regional metamorphism strikes generally northwest and dips steeply to the west. Foliation in the mineralized zone is predominantly flow-shear cleavage, which is intimately related to faulting. Intersection of cleavage directions commonly results in a lineation that plunges 35° to 80° southeasterly and in some places appears to control localization of the ore.

Major faults form three distinct sets that have strikes of N.60°W., N.45°W., and N.20°W., respectively, and dips that are steep to the west or vertical. The most prominent fault is the Kutam fault; it strikes N.60°W. and sharply bounds both the ore body and a broad zone of intensely sheared rock, known as the Kutam shear zone, on the southwest side.

The Kutam ore deposit is less distinctly bounded on the northeast by a barren zone of intensely silicified quartz porphyry, which probably formed by replacement of normal quartz porphyry during a hydrothermal, propylitic phase of pre-ore alteration. Brecciated silicified zones healed by later quartz are commonly associated with mineralization. Overall, the silicified rocks are more resistant to erosion than others and are probably in part responsible for the topographic expression of the ore deposit as a ridge, in contrast to adjacent less resistant zones of pyritic alteration, which occupy low-lying areas along strike in the principal shear zone. Most of the

ore occurs in highly sheared quartz porphyry that has been transformed to a quartz-sericite schist. Chlorite is locally abundant. Mica and chlorite replace hornblende, epidote, and plagioclase. Large masses of chlorite schist unaccompanied by considerable quartz and white mica probably formed directly by replacement of hornblende and epidote in rocks of the mafic volcanic sequence during a thermal metasomatic stage of alteration that occurred prior to the hydrothermal, propylitic stage. It seems likely that potassium was introduced during this early alteration.

Primary sulfide minerals in the ore zone are chiefly pyrrhotite, pyrite, chalcopyrite, and sphalerite. These minerals range from wisps and streaks less than 1 mm wide parallel to the schistosity to massive chalcopyrite-rich veins 2 m or more in width. The veins are irregularly spaced at distances of from several centimeters to several meters, and tend to form families of veins separated by unveined rock. A major proportion of the sulfides occurs as small disseminated crystals. Copper and zinc are zoned, and sphalerite diminishes in abundance toward the footwall of the deposit. To the northwest and southeast of the deposit along strike, pyrite is the predominant sulfide.

Iron oxides (hematite and goethite) locally form stockworks, especially in the northern part of the mapped area where they were probably derived from pyrite. Pyrite is abundantly disseminated in fresh cores from drill holes in this region. In general, oxidation has not penetrated to a depth of more than about 20 m from the surface. Malachite is the predominant copper mineral in the oxidized zone. Supergene sulfide minerals are lacking, probably because of the absence of sufficient pyrite to effect leaching of sulfides in the ore zone.

The geologic relations and ore occurrences are displayed in vertical sections along drill holes shown on plate 4 (reproduced from Smith and others, 1976). All sections have been plotted on a single map sheet at 1:4,000 scale beneath the trace of the surface projection of the corresponding drill holes in order to facilitate direct comparison with geophysical maps. Schematic representations of ore reserve blocks from Smith and others (1976) are shown on plate 5, both in plan (projected to the 2000 m level, which is 60-100 m beneath the surface) and in vertical section parallel to strike. The reserve estimates were made by Smith following standard procedures based on assays of ore intersections in the eight drill holes. Indicated and inferred reserves total 8 million tons containing 1.83 percent copper and 0.95 percent zinc.

It is now known from the combined results of drilling in the USGS and Noranda exploration programs (D. Bent, oral commun.) that the richest ore concentrations occur as rod- or pod-like bodies plunging steeply to the south or southeast.

ELECTRIC LOGS

Single-point resistivity and self-potential logs were made in several diamond drill holes at Kutam by means of a Neltronic Type D Logger (Model 1K). This instrument measures changes in alternating current resistance and self-potential in the immediate vicinity of a logging electrode as it is raised up through a fluid-filled borehole by a hand-cranked cable, using a ground electrode embedded in mud at the surface a few meters away from the hole collar as a reference point. The measured resistance, in ohms, between the two electrodes--that is, the grounding resistance of the downhole electrode--is related to the apparent resistivity by a geometric factor having the dimensions of length. In the case of a long cylindrical electrode such as that used with the Neltronic apparatus, the geometric factor K is approximately given by:

$$K = 2.73 \frac{L}{\ln 2 L/d} ,$$

where L = length of the electrode, d = its diameter, and the measured resistance equals K times the apparent resistivity (Keller and Frischknecht, 1966, p. 66). The apparent resistivity is strongly influenced by the true resistivity in the vicinity of the probe but will be close to it in absolute terms only under ideal circumstances. Therefore single-point resistivity and SP logs are normally used qualitatively and primarily for lithologic correlation purposes. The resistivity log gives a good indication of mineralized zones in the hole by registering very low resistance in the presence of massive metallic sulfides. This information was used at Kutam to select sites for the downhole electrode in mise-a-la-masse induced polarization surveys, and also to compare the distribution of conductive zones in adjacent drill holes.

The electric logs of drill holes KA-1, KA-2, KA-3, and KA-4 are presented on plate 6, along with geologic logs (structure, lithology, mineralization) reproduced from Smith and others (1978). Relative SP scales (millivolts per inch of deflection on the strip chart) and resistivity scales (ohms per inch) were changed during the logging operation as indicated. Slant depths are given in meters. It was seldom possible to lower the logging probe to the base of a given hole because the holes became flatter with depth, and in the case of hole KA-4, the probe

lodged at a slant depth of only 97 m. Logging was done by Merghelani and Blank in November 1974 and February 1975, some months after each hole was drilled. Because of various operational problems the results were of less than ideal quality.

Small vertical offsets of the instantaneous SP trace with respect to the resistivity trace are present due to imperfect pen positioning, but it is apparent that a positive change in the SP response (deflection to the right) generally occurs wherever there is a decrease in relative resistivity (deflection to the left). When the probe passes into air at the water table near the top of each hole the resistivity increases sharply, as is to be expected, while the SP either increases to a new and generally greater constant value or remains steady at the previous value. Casing can also affect both SP and resistivity levels. Normally no useful information is obtained above the water table.

Zones of mineralization are characterized by large and rapid fluctuations of resistivity, and sharp minima appear where the probe contacts stringers of sulfide. The fluctuations of SP are considerably smoother, and the SP logs are therefore easier to use in assessing the overall electrical behavior of a particular zone or formation.

For purposes of comparison all four SP logs are shown on figure 2 after replotting at a uniform sensitivity. They are arranged left-to-right in the order of the northwest-to-southeast distribution of the drill holes, and in addition, the log of KA-4 is plotted bottom-to-top instead of top-to-bottom, because this hole was drilled to the southwest in contrast to the other three. Each plot then represents an electrical sample of the quartz porphyry section from hanging wall to footwall of the ore zone. It can be seen that features of the SP logs for KA-1 and KA-2 can be correlated, even though the holes are separated by a distance of about 440 m. Neither set of logs shows much resemblance to logs of KA-3 and KA-4 although the shape of the KA-3 log does resemble that of the first two; KA-4 was not logged deep enough to make a valid comparison. Possible correlation zones are shown by dashed and queried connections.

The similarity of the KA-1 and KA-2 logs is due primarily to a similarity in disposition of sulfide concentrations in the two holes. This implies that the zones of massive sulfide ore are continuous along strike for at least the distance between KA-1 and KA-2 and that the strike-normal control of mineralization has been persistent through this distance. Such control could be stratigraphic or structural. In the absence of any evidence for

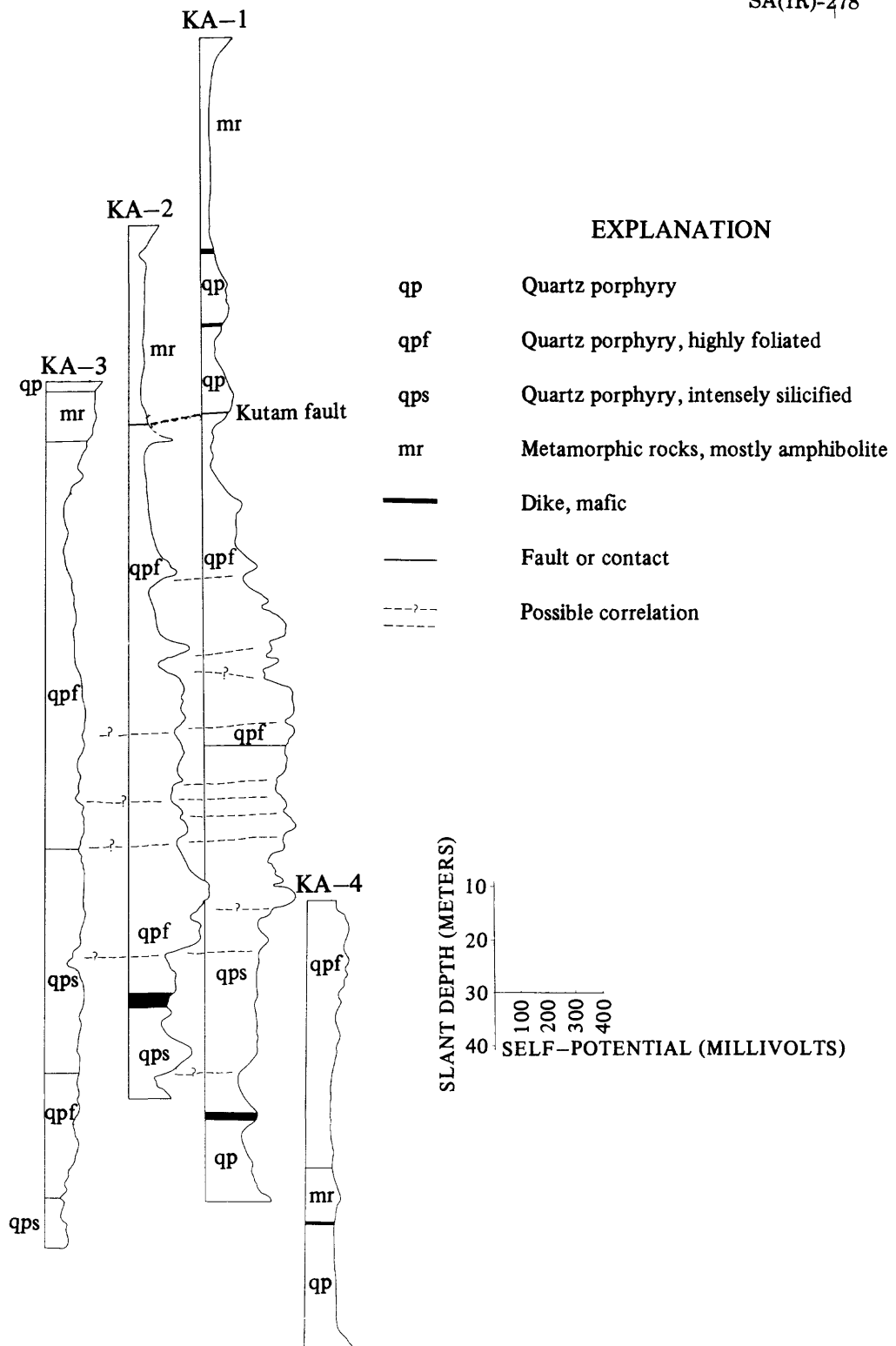


Figure 2.— Comparison of self-potential logs of drill holes KA-1, KA-2, KA-3, and KA-4, Kutam mine, Kingdom of Saudi Arabia .

detailed structural variations within the Kutam shear zone that could account for variations in intensity of mineralization across strike, it is suggested that the electric log correlations reflect primary lithologic variations and hence support the interpretation of an extrusive origin for the quartz porphyry.

RADIOMETRIC SURVEY

The purpose of the radiometric survey was to delineate surface concentrations of potassium in the altered zone, which might reveal a pattern of potassium metasomatism related to sulfide mineralization. The survey was carried out by Flanigan and Merghelani in March 1974 using an Exploranium model DISA-300 gamma-ray spectrometer. This instrument is the threshold, or integral, type and is capable of recording gamma radiation in four ranges. In the total count mode, all events of energy above 0.1 million electron volts (Mev) are recorded; in the potassium mode, all events above 1.3 Mev, in the uranium mode, all events above 1.6 Mev, and in the thorium mode, all events above 2.5 Mev are recorded. Therefore the potassium channel records energy peaks corresponding not only to K^{40} disintegration but also to that of Bi^{214} (uranium) and Tl^{208} (thorium), as well as all intervening peaks and normal background radiation (including cosmic rays and Compton scatter).

Readings were taken at 40-m intervals along the northeasterly grid lines. Events recorded on the potassium channel are displayed on the radiometric anomaly map of plate 7. A belt of potassium-channel highs oriented more or less northwest can be seen within the shear zone, and the maximum count rate exceeds 150 counts per second at one place over the ancient workings, as compared with a background count rate of 25-50 cps. The highs are irregularly distributed but in general seem to be associated with faults parallel to but northeast of the Kutam fault. Local orientations of anomaly axes give some indication that structures with more northerly trends have also influenced the potassium distributions.

The instrument used in this survey was calibrated against specimens that have chemically determined potassium concentrations, and it was found that a change in the count rate from 50 to 150 cps in the potassium channel represents a change in potassium content from 2.5 percent K_2O to 4.0 percent K_2O . On the assumption that other factors are constant, therefore, the observed range of gamma response of about 125 cps represents surface concentrations of about 2:1. The significance of the highs is open to question, particularly in view of the limited scope of the survey, but their existence suggests that potassium metasomatism was actively associated with mineralization processes.

SELF-POTENTIAL SURVEYS

The self-potential method involves measurement of the spontaneous electrical potential difference between a reference base station and other points on a survey grid or profile. Differences of potential can arise where a variation in oxidation state exists between different parts of a conductive ore body, so that in effect a voltaic cell is established and a system of electric circuits is set up through and external to the deposit. The resulting SP values can amount to a volt or more but are generally measured in millivolts (mv), and over the top of a buried ore body are always negative with respect to the surroundings. They can be detected by means of porous pot electrodes connected to a precision electronic voltmeter, or, if the electrode resistance is not very great, to any voltmeter having a millivolt range. Readings are sometimes affected by telluric currents, and on a much longer time scale, by changes of surface resistivity due to varying moisture conditions (Corwin and Hoover, 1979). Also, very large SP anomalies are commonly associated with graphite, and can be produced by electrofiltration, streaming potentials, and other phenomena that may have nothing to do with oxidation of sulfides.

The choice of a reference potential is entirely arbitrary, but a base station is usually located for convenience of access and in a non-mineralized environment. In the two-pot method of surveying, measurements are made of the potential difference between a stationary baseline electrode and a mobile electrode progressively advanced along a traverse line; baseline stations are then tied to the reference base. An alternate technique, the so-called "leap-frog" or three-pot (gradient) method, circumvents the need for deployment of long cables but has the disadvantage that errors can be cumulative.

All data for the Kutam surveys have been reduced with respect to an assumed zero potential datum at geodetic station B. Segments of the survey were carried out using different methods, at widely separated times, and under very different conditions of surface resistivity. Flanigan in March 1974 used the 2-pot method along northeasterly grid lines at 20-m station intervals; Merghelani, in February and May 1975, extended the coverage by both 2-pot and 3-pot methods following east-west grid lines and recording at 40-m intervals. The latter work was repeated in November 1976 by M. A. H. Bazzari. Internal inconsistencies between these surveys were as high as 50 mv, but the major anomalies are probably adequately delineated.

The results have been displayed as an equipotential map at a 25 mv contour interval (pl. 8). It appears that the choice of geodetic station B as a reference base was appropriate. A strong northwest-trending negative anomaly more than 500 m in strike length coincides very closely with the zone of ancient workings in the principal shear zone. The lowest SP value (maximum negative anomaly), -335 mv, occurs near the southeast end of the drilled deposit at the principal open pit near geodetic station D. A comparison with the plot of ore reserve blocks on plate 5 shows that most of the known or inferred ore is encompassed by the -50 mv closed contour (the northeasterly displacement of the SP anomaly with respect to ore reserve blocks is due to the southwesterly dip of the tabular ore zone). The negative anomaly becomes narrower and weaker towards the northwest, and exists only as a narrow trough over the thin ore zone penetrated by drill hole KA-3, beyond which it disappears. In the vicinity of each of the two minima of the anomaly, and especially of the weaker one (-125 mv closed contour near KA-2), the overall anomaly trend of about N.45°W. shows northerly perturbations. Southeast of the stronger minimum the anomaly decays abruptly.

These relations suggest that the prominent SP anomaly is indeed produced by voltaic effects associated with the ore body, that the ore zone has a steep southeastern termination--perhaps it is faulted or plunges steeply within the shear zone--and that it has an internal fabric controlled by the N.20°W. fault set.

A belt of relatively weak SP lows extends southeast of the mine along the projection of the Kutam shear zone. Minor pyritic alteration is present, particularly between KA-4 and KA-8, and as will be discussed in the following section, an intense Turam electromagnetic anomaly also occurs in this region. However, the SP values are all very positive with respect to the anomaly of the drilled ore body (immediately southeast of the ore zone they are positive with respect to the reference station), and probably do not merit further pursuit as ore indicators.

A large but ill-defined area in the southwest corner of the map is more than 50 mv negative, and minima exceed -75 mv. This area is also the locus of an induced polarization anomaly. No evidence of alteration was seen in bedrock exposures, but very little of the area has been mapped in detail and much is covered by wadi deposits. If the source of the anomaly is massive sulfide ore it must be deeper than the known ore zone; alternatively the anomaly could be due to a weak, broad, near-surface source. The source may in fact be graphite,

although the only known extensive outcrops of graphitic schist in the survey area (near the collar of drill hole KA-8) seem to have no effect on the trend of equipotential contours.

One of the most conspicuous features of the SP map is the east-trending discontinuity south of the ancient workings. The discontinuity does not coincide with any known geologic feature, nor have any structures of similar trend been recognized in the southern half of the map area. The SP data indicate that some sort of structure must be present here, and this inference is supported by the existence of similar trends in the distribution of other geophysical parameters. The question of trend significance will be discussed more fully in the concluding section.

TURAM ELECTROMAGNETIC SURVEYS

Turam, an acronym derived from Swedish words meaning "two-frame", is a fixed source, moving receiver method of electromagnetic prospecting involving measurement of relative phase shifts and amplitude ratios of the signals detected by two cable-connected, vertical-axis receiver coils ("staffs"), deployed at a constant separation at successive positions along lines crossing the strike of the target of investigation. The primary energy source is generally a long straight wire grounded at either end and positioned parallel to the strike but at some distance removed from the target, or alternatively, a large rectangular loop with sides parallel and perpendicular to the strike of the target. In the first case an EM induction field is generated that over an infinitely resistive earth decreases in amplitude as the linear inverse of perpendicular distance from the wire, except in the vicinity of the grounded ends. In the case of a rectangular loop the undisturbed field strength can be calculated by taking the vector sum of the fields due to the four straight line segments. It decreases more rapidly with distance than in the case of a long straight wire; at very large distances, the fall-off approaches that of a dipole field (decaying as the inverse cube of distance). Using the hypothetical undisturbed field strength values, the "normal" amplitude ratio for any position of the receiver pair can be readily obtained. However, if a conductor is present in the vicinity of the receivers, eddy currents will be induced in the substrate and the resulting secondary fields will distort the normal amplitude ratios and also produce relative phase shifts. A Turam system measures, in effect, the horizontal gradients in amplitude and phase of these secondary fields. In general, the better the conductor the larger the ratio and phase

anomalies (for a perfect conductor, however, the secondary field will be 180° out of phase with the primary field and no phase anomaly will be registered).

To facilitate the recognition of amplitude anomalies, it is standard procedure to "reduce" the measured amplitude ratios to a percentage of the normal ratio calculated for each position of the receiver pair, that is,

$$R_d = R_f/R_n \times 100,$$

where R_d is the reduced ratio, R_f is the ratio actually measured, and R_n is the calculated normal ratio. If a long straight cable is used as the primary source, then R_n is the inverse ratio of distances from the cable along any traverse perpendicular to it.

Measurements at two or more frequencies are commonly made in order to help evaluate the effect of conductive overburden. The "skin depth" (depth at which the surface amplitude of an EM wave is attenuated by $1/e$, or about 37 percent) is inversely proportional to the square root of frequency, and therefore in the presence of conductive overburden the fall-off in response to lowering of frequency will be rapid, whereas the opposite may be true if the response is due to a deeply buried conductor.

For some years Turam seems to have been the most commonly applied method of EM exploration on the Arabian Shield. A long grounded cable has been favored over a loop source, probably because of the simplicity of field operation and reductions, relatively slow decay of field strength with distance from the cable, and relative insensitivity to large topographic variations. On the other hand when a grounded source is used the possible non-uniformity of the galvanic return current system must be considered, in addition to the purely inductive secondary fields, and this added complication in data interpretation may more than offset such advantages because of the uncertainties involved.

At Kutam the system employed was an ABEM Turam model TS-4 and a grounded straight wire current source energized at 660 and 220 Hz by a 2.5 KVA motor generator. Flanigan and Merghelani in their survey of March 1974 over the northern part of the area used a cable 2 km long and oriented N.30°W., parallel to and 50 m southwest of their grid base line, which as we have seen was laid out approximately parallel to the strike of the mineralized shear zone. Readings were taken at 20 m intervals with the two receiver staffs spaced 20 m apart and moved along northeasterly traverse lines. The primary cable for the supplementary survey by Merghelani and Blank in November 1974

over the southern part of the area was 3.2 km long and oriented north-south, approximately along grid line 20E, with the northerly grounded electrode located near the collar of drill hole KA-3. It was later determined that KA-3 is in a zone of high near-surface conductivity; the proximity of the northerly grounded electrode to a shallow conductive zone may have resulted in a concentration of galvanic currents that contributed in a significant way to the Turam response, a point to which we shall return later. Readings using this source cable configuration were taken along east-west lines at 40 m station intervals and with 40 m receiver separation (the traverses crossed the strike of the shear zone at an acute angle). On lines 17S and 18S, both station interval and receiver separation were shortened over the principal anomaly to improve resolution.

Turam reduced amplitude ratio maps and phase difference maps at 660 Hz and 220 Hz, and location of the source cables for the northern and southern surveys, are shown on plates 9-12. For uniformity the March 1974 data (northern survey) have been presented at a receiver separation of 40 m instead of 20 m as used in the field. Likewise, the data for shorter spacings on lines 17S and 18S have also been presented at the standard 40 m separation. The method used in calculating reduced ratios and phase differences that would be observed at a separation larger than the one actually employed in the field differs somewhat from the conversion procedure recommended in the ABEM instruction manual, and is fully explained in the appendix to this report. On the amplitude ratio maps, the values contoured are reduced ratios of vertical field strength detected by the rear receiver (the receiver closer to the source cable) to that detected by the forward receiver (the receiver farther from the source cable), expressed as percent. The values contoured on the phase difference maps are phase lead of the field detected by the forward receiver over that detected by the rear receiver. Contour intervals are 5 percent and 1 degree, respectively.

Neither amplitude ratio nor phase difference isopleths for the two different surveys at 660 Hz (pls. 9 and 10) agree very well in the area of overlapping coverage, in spite of the use of a standard receiver separation. The discrepancies are due to the difference in source cable layout and hence in both induction fields and return current pathways.

Unfortunately the lower frequency section of the transmitter was inoperative during the March 1974 survey and the northern part of the prospected area, including the ancient mine, is covered by data recorded at the higher frequency only. Where anomalies at 660 Hz and 220 Hz can be compared (pls. 9 and 11 for amplitude ratio; pls. 10 and 12 for phase difference), they

are nearly identical. Lack of a frequency dependence is characteristic of anomalies due either to magnetic permeability response, or to galvanic current concentrations and/or eddy currents induced in a very large region. The shear zone is known from ground magnetic surveys to be essentially non-magnetic, as will be seen in a later section, and the anomalies are sharply localized. They are therefore probably largely due to galvanic current gathering in shallow conductive zones. Differences in phase results are much larger than differences in amplitudes at the two frequencies, which is in agreement with this interpretation.

Examination of the group of Turam maps shows immediately that 1) the electromagnetic field is not strongly disturbed over the ancient mine, and 2) two very prominent, more or less linear phase and ratio anomalies are present in the Kutam shear zone, disposed on either side of the drilled ore body. These two anomalies have nearly parallel axes but are not colinear. Their wavelengths, as well as those of other, less prominent Turam anomalies seen on the maps, indicate that the depths to their corresponding current concentrations are relatively shallow, in fact more or less comparable to the depth to the water table.

In order to facilitate interpretation of the principal anomalies and to compare them with the electromagnetic response of the ore zone, profiles of Turam parameters have been computed for traverses across the anomaly maxima and across the ancient mine (figures 3-6). The traverses selected are along lines 200N and 240S of the Flanigan and Merghelani survey and 18S of the Merghelani and Blank survey. Their locations are indicated on the Turam maps. The profile parameters are reduced amplitude ratio (in percent), phase difference (in degrees), and real and imaginary (in-phase and out-of-phase, or quadrature) components of the vertical field expressed as percent of the field at the receiver position nearest the source cable, where the field is assumed to be undisturbed and hence entirely in phase with the primary. (Real and imaginary components are obtained from values of the amplitude and phase at successive positions along the traverse, relative to the undisturbed field at the starting point. It can easily be shown that the amplitudes are obtained by successive divisions by the reduced field amplitude ratios, and the phases by algebraic addition of successive phase differences.) Each anomaly will now be discussed in the light of its map representation and the appropriate set of profiles.

The northern anomaly (pls. 9 and 10; fig. 3) has a total strike length in excess of 400 m. For about 160 m of this distance the amplitude ratio exceeds 125 percent. The axis of

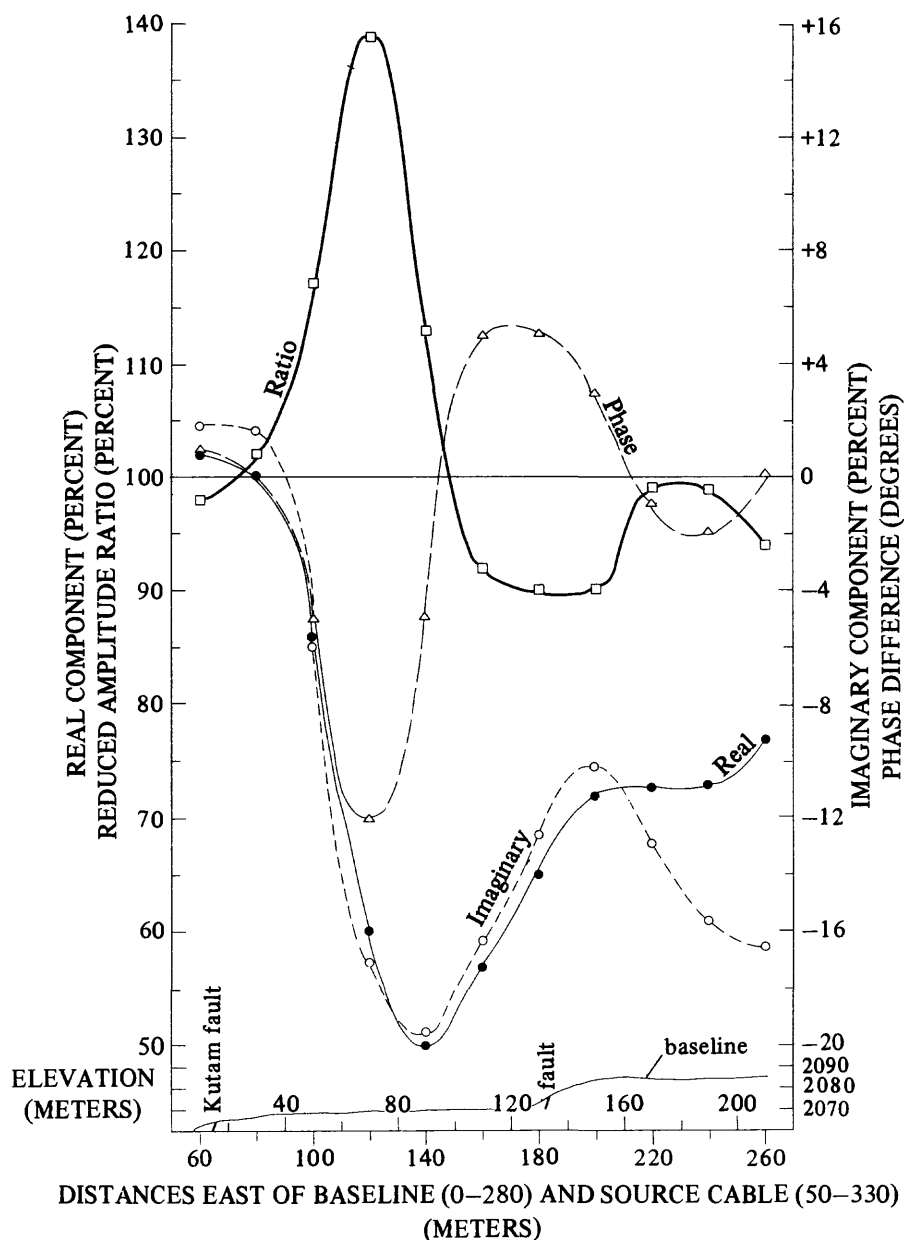


Figure 3.—Turam profiles, line 200N (660 Hz), Kutam mine, Kingdom of Saudi Arabia. Reduced amplitude ratio (open squares) expressed as percent of vertical EM field at forward receiver sensed at rear receiver; relative phase difference (open triangles) expressed as degrees of phase lead of field at forward receiver over that at rear receiver; real (in-phase) and imaginary (quadrature) components (solid and open circles, respectively) expressed as percent of field amplitude at rear-most receiver position (portion nearest source cable). Receiver coil axes in vertical mode. Data from Flanigan and Merghelani survey of March 1974, recomputed for 40-m receiver separation. For location of profile and grounded source cable see plates 9 and 10. Faults indicated on accompanying topographic profile taken from plate 3.

the anomaly is centered between major boundary faults of the Kutam shear zone, and the axial trend is nearly that of the zone, although in the northwest there seem to be two convergent axes of the ratio anomaly, and in the southeast (near the northern limit of the ancient workings) the axial trend of the ratio anomaly swings approximately north as the anomaly weakens. The maximum ratio and phase anomalies are 139 percent and -12° , respectively. Depth of the associated current concentrations, estimated from the half-amplitude width of the ratio curve (fig. 3), is slightly less than 34 m in the vicinity of the maximum; and their location, taken as the inflection point of the real and imaginary component curves, is about 40 m east of the Kutam fault. Because of the possibility that the response has been strongly affected by galvanic currents, quantitative interpretation of the profiles based on comparisons with inductive response from thin sheet models probably is not justified.

Bedrock in the vicinity of this anomaly is partly concealed by tailings from the ancient excavations, but clearly has been subjected to extensive shearing and alteration. Typically the rock has weathered to a surface of low relief (see topographic profile for line 200N, fig. 3) and is stained rust-red or maroon; evidence of sericitization and impregnation with pyrite is abundant. Lithologies specifically associated with the high conductivity are unknown. The anomalous source should have been intersected by drill holes KA-7 and KA-3, neither of which encountered more than disseminated mineralization (largely pyritic) beneath the anomaly axis (see plate 4; refer also to plate 6, electric log of KA-3). However, the geochemical survey revealed that a belt of scattered copper and zinc anomalies extends northwest from the ancient mine (pl. 2).

The southern prominent Turam anomaly (pls. 9-12; figs. 4, 5) has a total strike length in excess of 500 m. At its northwest end it is a weak anomaly whose axis approximately follows a major shear fault that forms the footwall of the ore body. From about 100 m to 400 m southeast of the mine the intensities of the phase and amplitude response are greatly increased and the axial trend is slightly more southerly than that of the Kutam shear zone. The computed maximum amplitude ratios are 235 percent (660 Hz) and 222 percent (220 Hz); with corresponding phase differences of -20° (660 Hz) and -10° (220 Hz). These values are only about 80 percent of those that would have been obtained on a strike-normal traverse. The anomaly in this region, where the pattern of disturbance is confined within boundary faults of the shear zone, is the most intense feature detected by the Turam survey. Farther to the southeast the axial trend changes to southerly or even southwesterly as the anomaly weakens, as in the case of the northern anomaly discussed previously.

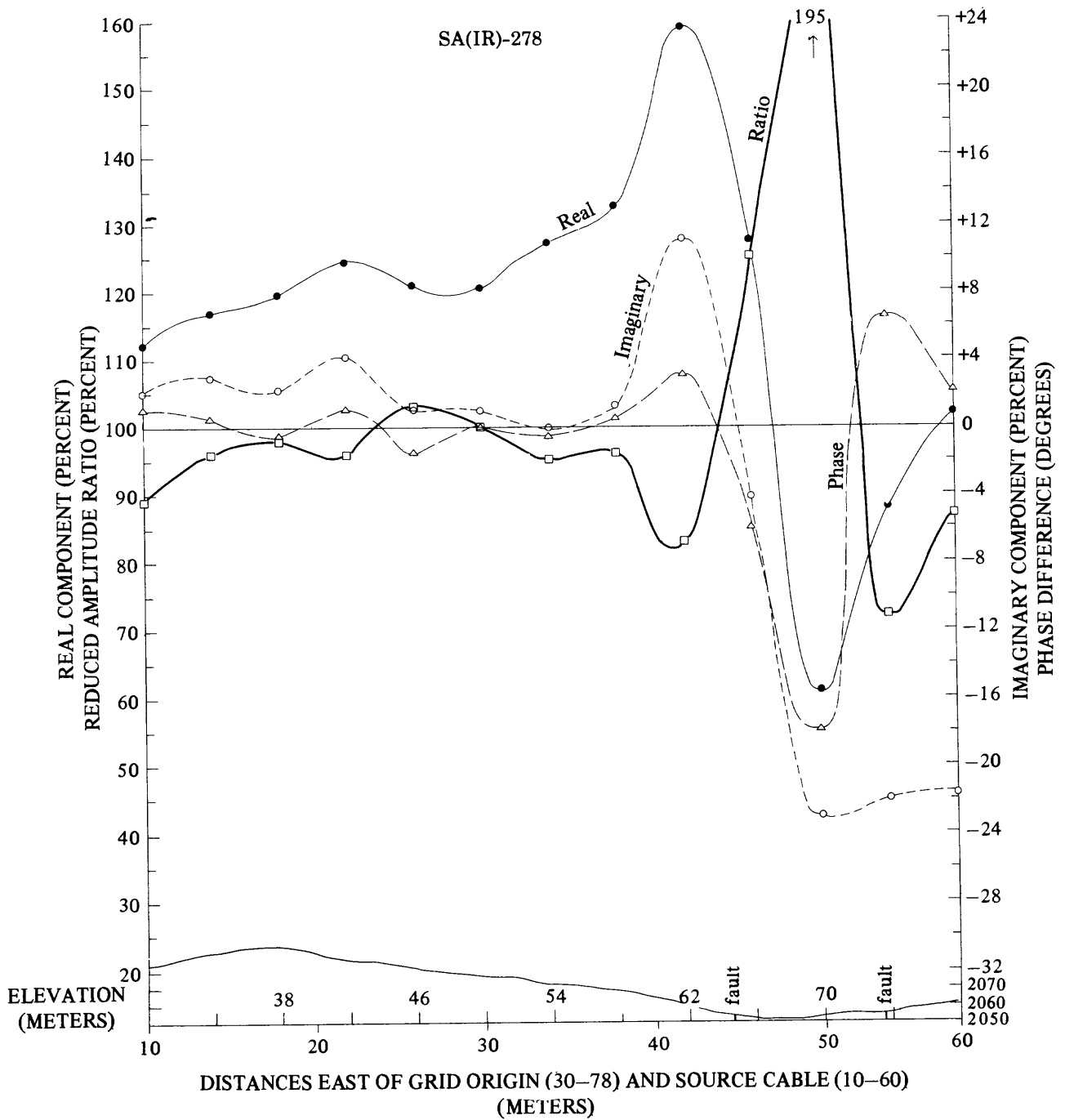


Figure 4.—Turam profiles, line 18S (660 Hz), Kutam mine, Kingdom of Saudi Arabia. Reduced amplitude ratio (open squares) expressed as percent of vertical EM field at forward receiver sensed at rear receiver; relative phase difference (open triangles) expressed as degrees of phase lead of field at forward receiver over that at rear receiver; real (in-phase) and imaginary (quadrature) components (solid and open circles, respectively) expressed as percent of field amplitude at rear-most receiver position (position nearest source cable). Receiver coil axes in vertical mode. Data from Merghelani and Blank survey of November 1974. For location of profile and grounded source cable see plates 9 and 10. Faults indicated on accompanying topographic profile taken from plate 3.

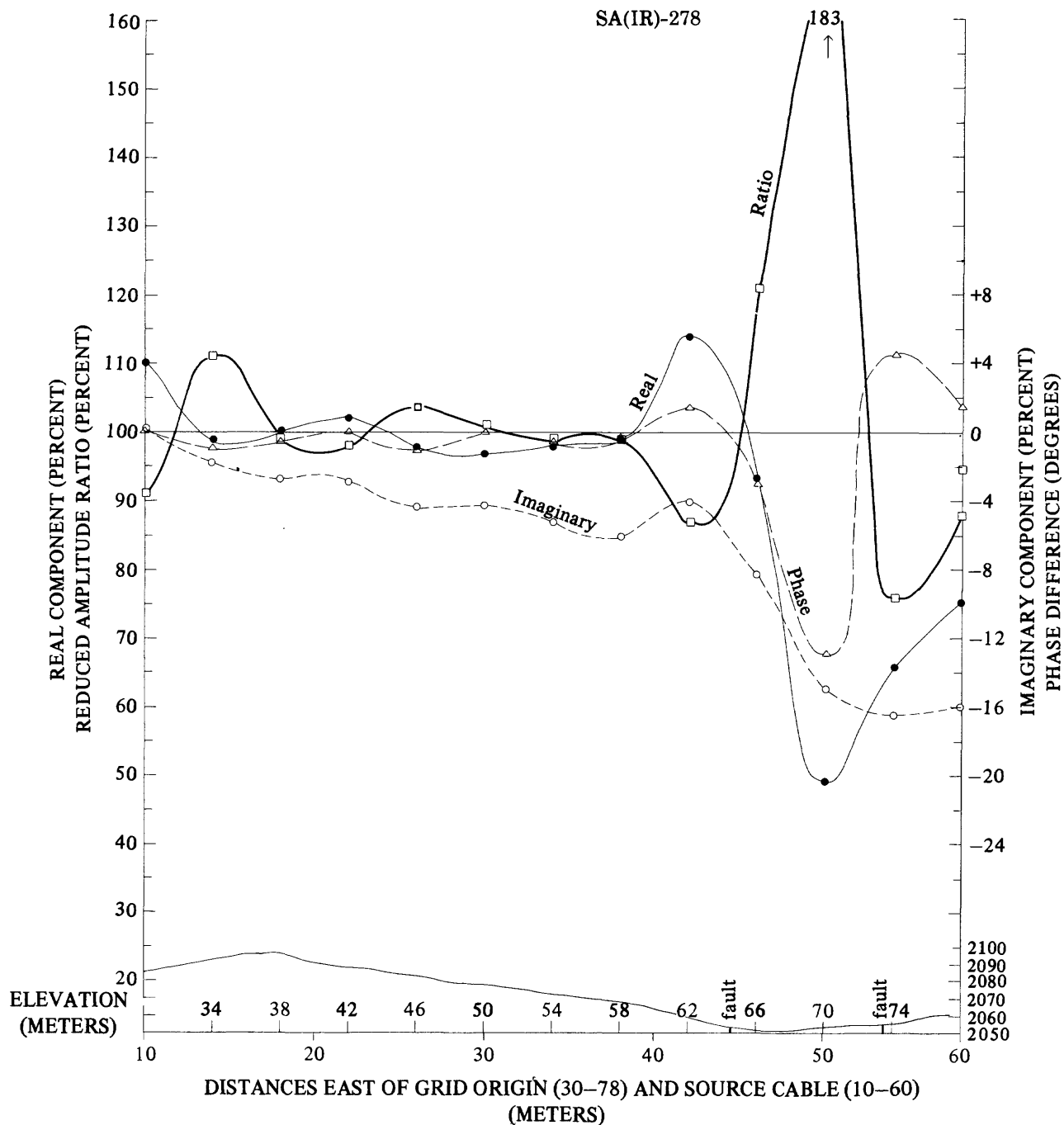


Figure 5.—Turam profiles, line 18S (220 Hz), Kutam mine, Kingdom of Saudi Arabia. Reduced amplitude ratio (open squares) expressed as percent of vertical EM field at forward receiver sensed at rear receiver; relative phase difference (open triangles) expressed as degrees of phase lead of field at forward receiver over that at rear receiver; real (in-phase) and imaginary (quadrature) components (solid and open circles, respectively) expressed as percent of field amplitude at rear—most receiver position (position nearest source cable). Receiver coil axes in vertical mode. Data from Merghelani and Blank survey of November 1974. For location of profile and grounded source cable see plates 11 and 12. Faults indicated on accompanying topographic profile taken from plate 3.

Progressive shortening of receiver coil separations during the survey of lines 17S and 18S established that the anomaly axis directly overlies an unimpressive zone of pyritic alteration a meter or two wide in quartz porphyry. From the half-amplitude width of the ratio profiles, the depth of the current concentrations must be about 35 m, or about the same as for the anomaly northwest of the ancient mine. Drill hole KA-8 encountered minor chalcopyrite stringers where it passed beneath the anomaly axis at a vertical depth of 90 m, but essentially no mineralization was found in the portion of the shear zone transected at shallower depths west of the anomaly. No copper or zinc anomalies were found in this area by the geochemical survey.

Neither of the two major Turam anomalies described here is associated with a strong induced polarization effect, as will be seen in the following section. Both occur in weakly pyritized areas but it is unlikely that they are associated with more intense mineralization; indications of copper or zinc mineralization are weak or absent, according to the results of geochemical sampling, geologic mapping, and diamond drilling carried out in the vicinity thus far. However, both anomalies occur in low-lying segments of the Kutam shear zone, both are associated with shallow current concentrations at or slightly below the water table, and as will be shown, both occur in regions of near-surface high conductivity mapped by the IP survey. It has already been pointed out that the anomalies probably represent to a large degree the effect of galvanic current-gathering as well as that of induction.

From these considerations, it appears that the two most prominent Turam anomalies may reasonably be attributed to ionic conduction, perhaps enhanced by surface conduction in clay minerals, in the pyrite-impregnated, propylitically altered and water-saturated rock of the Kutam shear zone. Dikes, faults, or other structures which can serve as electrolyte barriers or channelways may also have altered the conductivity distributions in the near-surface environments. Judging from trends within the two main anomaly systems as well as those of other anomalies seen on the Turam maps, conductivity anomalies probably reflect to some extent the influence of northerly-trending structures as well as that of the shear zone. Abundance of weathered pyrite seems to be associated with production of the strong ionic solutions postulated to account for the observed Turam response.

Turam profiles for a traverse across the ore body (line 240S, Flanigan and Merghelani survey) are given on figure 6. A weak response is evidenced, but the maximum ratio over the ore is only about 110 percent, the anomaly is very broad and diffuse, and it merges with the weak northwesterly extension of the major anomaly discussed previously. One must conclude that the Kutam ore body as a discrete Turam target was essentially not detected.

That no substantial Turam anomaly occurs over the Kutam ancient mine is somewhat surprising in view of the drilling results, which indicate the presence of a multi-million ton massive sulfide ore body beneath the zone of ancient workings. This fact must relate not only to the total mass of the ore but also to its mineralogy (the sphalerite component, for example is non-conductive), to its structural characteristics, to the electrochemical environment, and perhaps also to the physical parameters of the EM survey.

From the relative strength of ratio and phase anomalies the source of the very weak disturbance over the ore zone is inferred to be highly resistive. The bulk resistivity of ore and gangue minerals may simply be too high for a satisfactory EM target; but it is known qualitatively from the electric logs and quantitatively from the induced polarization surveys that resistivities in the ore zone are not prohibitively high. A possible explanation of this apparent contradiction is that the mineralization is distributed in such a way as to present a minimum induction target for the particular surveying layout employed. A tabular conductor dipping toward the source cable should in theory give no response at all if the dip is such that no magnetic flux cuts the conductor. This condition may have been approached in the Kutam survey. Moreover the principal ore concentrations are known to be somewhat rodlike and steeply plunging, rather than sheet-like, and they may in general be poorly interconnected so that optimum coupling could be doubly difficult to achieve. As a whole the Kutam ore body evidently presents a less than ideal EM target. In any case it would be advisable to pursue the Turam investigations using a source cable--preferably a rectangular loop--located to the east of the deposit, where the terrain is more resistive and the aspect more favorable. The Turam method should be supplemented by other EM methods such as slingram or shootback, before a final evaluation of the effectiveness of EM in this environment is made.

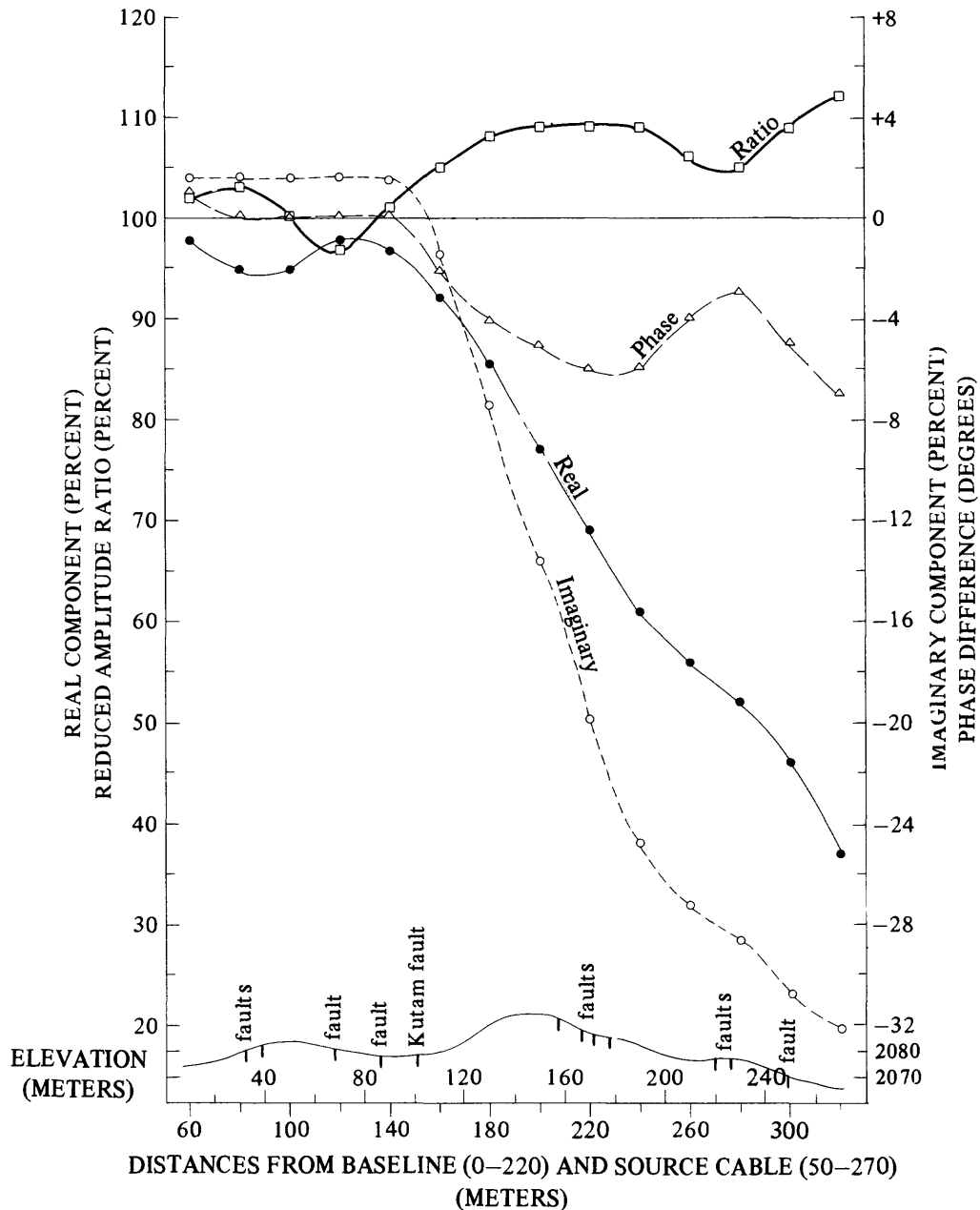


Figure 6.—Turam profiles, line 240S (660 Hz), Kutam mine, Kingdom of Saudi Arabia. Reduced amplitude ratio (open squares) expressed as percent of vertical EM field at forward receiver sensed at rear receiver; relative phase difference (open triangles) expressed as degrees of phase lead of field at forward receiver over that at rear receiver; real (in-phase) and imaginary (quadrature) components (solid and open circles, respectively) expressed as percent of field amplitude at rear—most receiver position (portion nearest source cable). Receiver coil axes in vertical mode. Data from Flanigan and Merghelani survey of March 1974, recomputed for 40-m receiver separation. For location of profile and grounded source cable see plates 9 and 10. Faults indicated on accompanying topographic profile taken from plate 3.

If the northern and southern prominent Turam anomalies are largely due to galvanic current concentrations in ionic solutions, why was a similar phenomena not observed in the vicinity of the ancient workings? The answer to this question may involve fundamentally the contrast of alteration minerals present in the ore body with those in adjacent regions of the shear zone. It can be speculated that the more strongly pyritized and sericitized zones produce more strongly ionized groundwater on the one hand, and that the rock is more pervasively wetted where it is less silicified, on the other. On the average the depth to water table in the ore zone is about 10 m greater than in the adjacent segments of the shear zone, which have been more deeply eroded and lie at or near the level of the trunk wadis. Whatever the explanation, the galvanic response of the silicified and high standing ridge of the ancient workings was apparently minimal.

One additional remark is in order before leaving the discussion of results of the Turam survey. The anomaly detected by Flanigan and Merghelani to the northeast of the Kutam shear zone, along the projection of drill holes KA-2 and KA-3 has reduced ratios that reach as high as 125 percent and phase differences of more than 17° , although the anomaly was not fully delineated and its maximum intensity may not have been reached. Its axis trends approximately north and it is more or less on strike with north-trending mineralized elements of the ore zone. The surface of the Precambrian beneath the anomaly is concealed by Wajid sandstone. Anomalous copper values were found on the nearest geochemical traverse (line 7S) (although this discovery is hardly surprising, as they occur where the traverse crossed the ancient workings). Finally, the Turam anomaly is loosely associated with mise-a-la-masse IP anomalies detected by means of two different electrode configurations. Because all of these indicators are favorable (though none compelling), the source of the anomaly is considered to have enough economic potential to place it on the roster of future exploration targets.

INDUCED POLARIZATION SURVEYS

Until the last several years relatively little induced polarization (IP) work had been done in the Arabian Shield, probably because the prime base metal exploration targets were considered to be "massive" sulfides, for which a strong electromagnetic induction response rather than a strong polarization response was predicted. The IP surveys in the

Kutam area were among the first on the shield and were therefore carried out on a quasi-experimental basis. The equipment used consisted of a Geoscience frequency-domain model T2800 transmitter and model R5280 phase-lock receiver, made available for this project through the courtesy of the Bureau de Recherches Géologiques et Minières (France). Geophysicists J-M. Georgel and D. Achard of BRGM generously assisted in setting up and carrying out the initial field operations.

In frequency-domain IP measurements the transmitter applies a square-wave pulse at two or more different frequencies (in this case 0.3 Hz and 3.0 Hz) to a set of current electrodes; the receiver measures the potential difference between successive points on a grid or profile at each frequency. Any geometrical array of the four electrodes can be selected, as in ordinary applied potential or direct-current resistivity measurements. The results are generally expressed as apparent percent frequency effect (PFE), apparent resistivity (ρ_a) at the lower frequency, and apparent metal conduction factor (MF). The metal factor is a supplemental parameter that has sometimes proved useful for characterizing ores such as the Kutam type that are neither purely disseminated nor purely massive, because both IP effect (chargeability, polarizability, or frequency effect) and resistivity enter its computation. It is related to the other two parameters as follows:

$$MF = A \left(\frac{\text{IP effect}}{\rho_a} \right),$$

where A is a numerical coefficient chosen to produce a satisfactory range of values. In the present report,

$$PFE = \frac{\Delta V_{f_1} - \Delta V_{f_2}}{\Delta V_{f_1}} \times 100 = \frac{\rho_{af_1} - \rho_{af_2}}{\rho_{af_1}} \times 100,$$

where f_1 , f_2 are lower and higher frequencies, respectively, and the ΔV 's are the measured differences of potential across the receiver dipole; and

$$MF = 2\pi \times 10^5 \times PFE/\rho_a,$$

where apparent resistivity is expressed in ohm-feet.

IP effects are manifested by a time lag required for a complete build-up or decay of an applied voltage. They can be caused either by electrode polarization, in which mineral grains impede the normal passage of electrical current by ionic

conduction in pore space electrolytes, thus creating a back-emf phenomenon known as "overvoltage", or by membrane polarization, in which the buildup of ionic charges on the surface of clay particles impedes the current. Many sulfide deposits are not very responsive to inductive methods of exploration but display a large IP effect due to the large aggregate surface area of metallic minerals. IP anomalies can also be obtained from bodies of clay, graphite, or any rocks rich in disseminated iron oxides.

Dipole-dipole

The mine area at Kutam was traversed by seven east-west dipole-dipole profiles; the dipole length was 40 m and spacing between source and receiver dipoles was from one to six dipole lengths. Vertical pseudosections constructed from these profiles are shown on plates 13, 14, and 15, for percent frequency effect, apparent resistivity, and metal factor, respectively. The pseudosections were constructed according to the standard procedure of plotting a value for a given configuration at the point of intersection of lines extending downwards from the center of each dipole at 45° angles (fig. 7). However, each section has been truncated at level N=1 on plates 13-15, and plotted such that the line of truncation coincides with the plan position of the profile; in this way all seven sections can be represented on one map without overlap. The truncation must be considered in extrapolating pseudosection features to the surface. It should be realized that pseudosections give a highly exaggerated impression of depth of exploration and also that the patterns produced are very different than the actual distribution of anomalous material in the subsurface. Nevertheless, results presented in this standard format can be used qualitatively, or can be compared with pseudosections from model experiments or with computer-generated pseudosections, as an interpretive aid. (For a general discussion of the use of pseudosections see, for example, Telford and others, 1976, p. 720-721.)

Examination of the PFE pseudosections on plate 13 shows that the maximum frequency effect found exceeds 7 percent and occurs on profile 9S, which crosses the drilled ore body. The background frequency effect (PFE in non-mineralized terrain) is generally less than 2 percent.

Profile 3S shows a surficial negative PFE anomaly at about stations 8E-12E, below which the PFE rises to more than +3. The source of the positive anomaly is probably a concentration of pyrite in the Kutam fault zone, and the associated negative

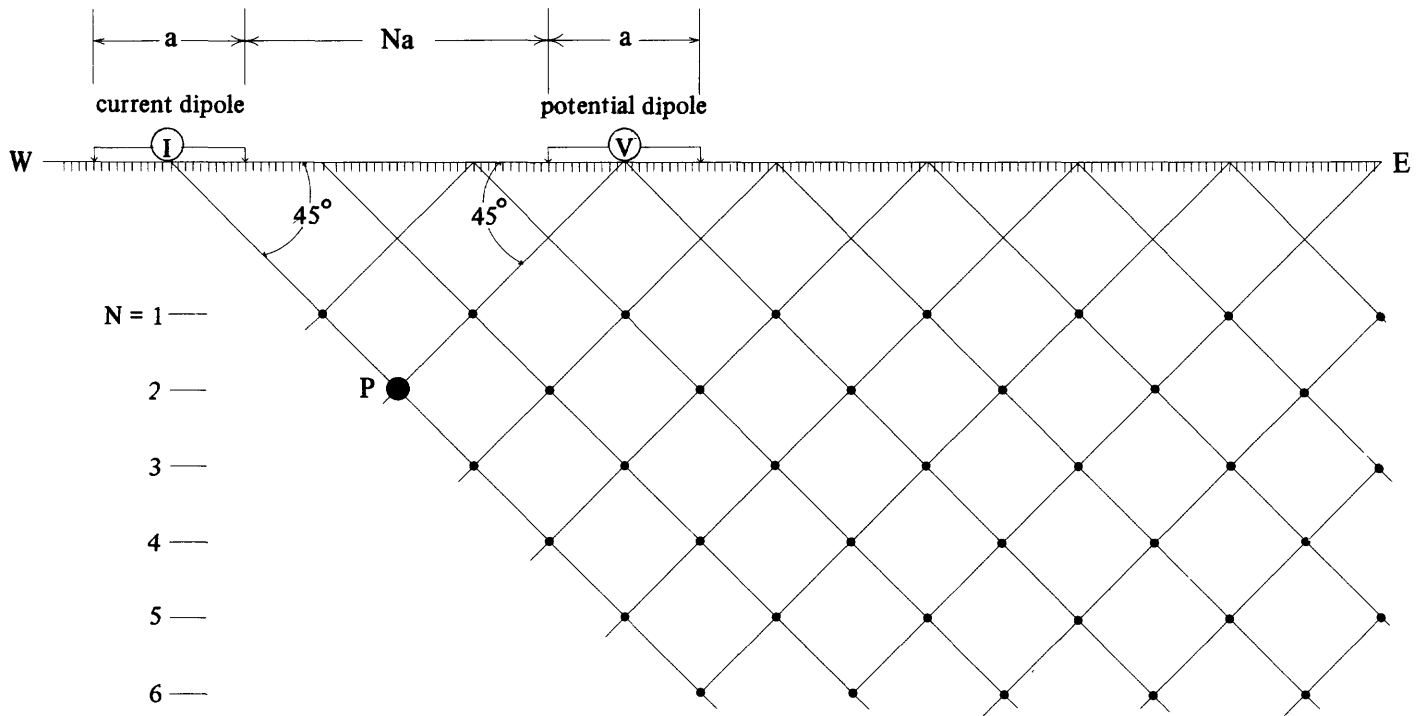


Figure 7.—Method of construction of dipole–dipole pseudosections, showing plot point P at west end of line, for $N = 2$. Dipole length $a = 40$ m for Kutam surveys and $N_{\max} = 6$.

anomaly probably arises from the geometry of the polarization discharge currents. This is not at all unusual where the polarized body has a high conductivity (see, for example, Sumner, 1976, p. 195-196 for a discussion of negative IP effects). Farther along the line a weakly polarizable zone is indicated at about 16E. This zone seems to be a strike extension of strong anomalies detected on profiles 6S, 9S, and 12S.

A negative anomaly of 3 PFE (3-5 PFE below background) is also found on profile 6S at about 0E, in barren quartz porphyry terrane. Its cause is unknown. The principal anomaly on this profile is that of a polarizable body dipping steeply to the west and reaching nearly to or to the surface at 26W-28W. This body is the ore zone encountered in drill hole KA-3. The frequency effect increases with depth.

Profile 9S shows a similar but much more intense anomaly due to a source of about two dipole widths (80 m) and steep westerly dip, with a surface trace centered at about 32 E (the maximum concentration of workings). On profile 12S the response is similar but not so intense; the trace has shifted to the east. The steepness and uniformity of the gradient in pseudosection reflect the Kutam fault on the western boundary of the ore body. At profile 15S the response has become more discontinuous, though just as intense as on the previous profile. The center has shifted farther east to about 46E. These four profiles, 6S-15S, give the expression of the drilled Kutam ore body--a thick tabular deposit of strike N.40°-45°W. and steep dip westerly.

No tabular source is evident on the pseudosection of profile 18S. However, this profile reveals two zones in which the PFE increases with depth to values exceeding 4. A resurvey of this profile at greater dipole lengths would be desirable because of the possibility that the mineralized zone is still present, though deeper and displaced westward. The profile does not extend far enough to the east to test fully the southeastern Turam anomaly zone.

Profile 21S shows that an IP response is indeed associated with the Turam zone, at about 72E, but the response is very weak and non-uniform. It is apparently due to pyrite mineralization in the Kutam shear zone. On the west side of this profile the PFE gradient suggests that a discontinuity has been crossed at about 28E and that a strongly polarized body is present to the west of the profile. There are no Turam data west of 30E because of proximity to the source cable. Without extending the IP dipole-dipole profile to the west, it is impossible to

estimate the shape or depth of the disturbing body. The maximum PFE value of 6, however, is similar to the maximum response of the Kutam ore body, and the area warrants further investigation. A local SP anomaly of -75 mv is also present in this vicinity. It is possible that this anomaly represents copper mineralization, but there is no geochemical support for subsurface presence of copper or zinc (see pl. 2).

Pseudosections of apparent resistivity shown on plate 14 yield several new insights concerning the subsurface distribution of mineralization. On these sections the areas with apparent resistivity less than 100 ohm-meters are shaded for emphasis; these favor the presence of high grade mineralization. Contours are at intervals of 0.25 on a logarithmic scale (10, 18, 31, 56, 100 ohm-meters, and so forth).

Profile 3S shows a superficial highly conductive zone ($\rho_a < 100$ ohm-meters) centered immediately east of the Kutam fault, at about 12E, and coincident with the northwestern Turam anomaly. The anomalous PFE source believed to reside deeper in the fault zone probably is not conductive. The apparent resistivity of the weakly polarizable source at 16E is high at the surface, but apparently decreases with depth.

Profiles 6S, 9S, and 12S reveal the main ore zone as a zone of relatively low apparent resistivity, but the lowest values attained are nowhere less than 20 ohm-meters (the true resistivity is of course unknown but could be much lower). The pattern is that of a complex source; line 12S, in particular, suggests the existence of two discrete steeply dipping low-resistivity zones, which represent either mineralization concentrated near the principal boundary faults of the Kutam shear zone, or, alternatively, perhaps water-filled permeable zones or clay minerals in this environment. The sharply defined eastern limit of the apparent resistivity anomalous zone of profile 12S is a mapped fault, which intersects the profile at about 52E (see plate 3). The minimum value of resistivity for these three profiles is reached on profile 9S about 100 m east of survey point B, in the region of maximum IP effect. This zone trends northwest and lies immediately east of the Kutam fault.

Profile 15S shows a highly conductive zone that may be an extension along strike of the eastern anomalous zone of the previous profile (12S). Both appear to be associated with the same fault, and both are on the flank of the strong southeastern Turam anomaly. Apparent resistivity values near the surface ($N=1$) on line 15S reach less than 10 ohm-meters, the lowest computed for any profile. Such low values are not surprising in view of the very strong Turam response in this region. The highly conductive zone was not detected on line 18S, probably because

that profile was not carried as far east as the axis of the Turam anomaly. Line 21S crosses the point of maximum peak response of the Turam anomaly, at about 72E--but the corresponding apparent resistivities are no lower than a few hundred ohm-meters. This seems to confirm that the source of the Turam anomaly here is a very good conductor of very small cross-section.

Profiles 15S, 18S, and 21S all show apparent resistivity decreasing with depth on the westernmost end of the profiles. This decrease need not be related to mineralization, but it reinforces the conclusion from PFE pseudosections and SP that the area should be examined further.

The metal factor pseudosections of plate 15 are very similar to the apparent resistivity pseudosections and therefore contribute little to an understanding of disposition of the ore zones. Such similarity is not unusual and is the reason why many geophysicists do not favor the use of metal factors. The pseudosections do show that metal factors in the Kutam ore zone exceed $10,000 \Omega^{-1}\text{ft}^{-1}$, which is generally the lower limit of the range of economic interest.

Mise-a-la-masse

Following the initial dipole-dipole tests, the east-west grid lines at Kutam were covered by a survey using the mise-a-la-masse IP technique. In mise-a-la-masse surveys one current electrode is inserted down a drill hole and positioned at a conductive zone in the ore body, as the name implies; and the other is normally situated at a great distance from the area to be surveyed so that it has very little effect on the potential distributions. Ideally the downhole electrode functions as an isolated point source. Depending upon the geologic environment, however, the potentials may in fact be somewhat influenced by the locations of the remote electrode, and therefore one or more alternative remote sites may be switched in for each set of potential measurements. Likewise alternative downhole electrodes may be used. In the latter case, the effect on potential distributions is commonly very drastic. Potential measurements for IP mise-a-la-masse surveys are made with two porous pots spaced a constant distance apart to record voltage gradients, either in time or in frequency domain; the overall configuration is thus in effect pole-dipole.

The downhole current electrode for the Kutam survey was placed in drill holes KA-1, KA-2, and KA-3 at slant depths of 190, 78, and 215 m (vertical depths of 120, 68, and 168 m) respectively, these positions having been selected on the basis of the electric log data for optimum contact with the ore

(minimum electrode resistance). In each case, the remote current electrode was positioned 2.5 km west-southwest of the mine, or more or less normal to the strike of the Kutam shear zone, in silty overbank deposits of Wadi Kutam some 200 m west of the exploration camp and 100 m upstream from a concrete highway bridge. At the onset of the survey, measurements were also taken using a remote electrode situated about 2.5 km to the south-southeast of the mine, more or less along the strike of the shear zone, but the results were so similar to those obtained with the western remote electrode that the former position was abandoned in the interests of time economy. The receiver dipole length was 40 m. Difficulties were encountered in grounding the receiver pots at some grid points over the mine excavations, particularly during the very dry month of November 1974, and readings were unstable at several additional points (16S, 54E using KA-2; 16S, 50E, 17S, 46E, and 17S, 50E using KA-3) for reasons unknown, but probably related to electrode grounding.

Reduction of the field data to yield the derived quantities, apparent resistivity and metal factor, were made with the assumption that the downhole current electrode is embedded in a uniform half-space at a depth given by the difference in elevation between that electrode and each point of calculation of potential. Then by the method of images it can be shown that the potential difference ΔV between two receiver electrodes is simply

$$\Delta V = \frac{I \rho_a}{2 \pi G}$$

where the geometric factor G is

$$G = \left(\frac{1}{R_1} - \frac{1}{R_2} \right) - \left(\frac{1}{R_3} - \frac{1}{R_4} \right),$$

in which R_1, R_2 are the distances from the near and far current electrodes to the first potential electrode, and R_3, R_4 are the distances from the near and far current electrodes to the second potential electrode (see, for example, Heiland, 1940, p. 712). In general $R_2, R_4 \gg R_1, R_3$. Because pot positions were grid points of the topographic survey, the R 's could readily be calculated. Except in the immediate vicinity of the downhole electrode, distortions introduced by variations of topography are negligible.

The IP mise-a-la-masse results are shown on plates 16-21. The first two maps give isopleths of percent frequency effect for the downhole electrode in drill holes KA-1 and KA-2 (pl. 16) and KA-3 (pl. 17). Values believed to be spurious and hence ignored

in the contouring are plotted on these maps but not on the maps of apparent resistivity and metal factor which follow (pls. 18-21).

Background PFE levels are seen to be in the range 0-5, and strong anomalies of both positive and negative sign are present. Also substantial differences between the two maps are noted: the anomaly patterns are clearly electrode-dependent. This dependence is related to the complexity of charging current pathways where highly conductive zones are intimately associated with the polarizable sources.

An extensive northwest-southeast-oriented anomaly system with positive amplitudes of 6-10 PFE and sharp associated negative anomalies is common to both maps and occurs over the principal mine workings (in detail this anomaly system, too, is electrode-dependent). The existence of a *mise-a-la-masse* anomaly over the Kutam ore body is in agreement with the dipole-dipole results and confirms that the ore body as a whole is highly polarizable. Moreover, the main elements of a very intense negative anomaly system immediately south and southeast of the mine are also seen on both maps, having been detected with all three downhole electrode positions. The cause of the negative response, like that of most negative IP anomalies in frequency-domain surveys, is not easily ascertained: a negative PFE implies that the IP charging current is opposite in sign to the steady-state current that would be obtained using the same current electrodes, and can be at least in part attributed to the geometry of the polarizable source, but a difference in electromagnetic coupling at high and low frequencies could also be a contributing factor. In the present case the northern part of the negative anomaly system is aligned sharply east-west and must in some way reflect the southeastern termination of the Kutam ore deposit. The negative PFE values could be related to the fact that the uppermost part of the ore zone stands well above the adjacent topography. It has not yet been possible to unravel the complex geometry and connections between conductive zones that give rise to this complicated negative anomaly system.

One important result of the *mise-a-la-masse* surveys, again in agreement with dipole-dipole data, is that only a weak IP response appears in the vicinity of the principal Turam anomalies to the northwest and southeast of the ore body. As we have seen, this is part of the argument for associating the Turam response there with ionic, rather than metallic, conduction. The disseminated metal content in these zones seems to be insufficient to produce an appreciable electrode polarization, and no evidence has been found of a massive metallic conductor for which little or no IP response could be expected, that is, a conductor with relatively low surface area.

That several strong anomalies appear on one but not the other of the two PFE maps is perhaps the result of large differences in the degree to which ore zones in KA-1, KA-2, and KA-3, are coupled to the other conducting zones. The anomaly centered on drill hole KA-7 on the KA-2 map (pl. 16), for example, is missing on the map made with the KA-3 electrode (pl. 17). KA-7 was started in altered and weakly pyritized rock, and up to 10 percent pyrite was encountered in this hole where it intersected the Kutam fault at 100 m depth, well to the west of the anomaly; KA-6 encountered up to 2 percent disseminated pyrite at a depth of 100 m slightly east of the anomaly (see vertical sections, pl. 4). These zones of pyritic enrichment, which are apparently the source of the anomaly, must be well coupled to the electrode in KA-2 but very poorly coupled to the electrode in KA-3. The mise-a-la-masse anomaly is only about 40 m northeast of the intense negative PFE anomaly and low resistivity zone of dipole-dipole line 3S, and the two probably have a similar origin.

A weaker, positive PFE anomaly unique to the map of plate 16 is centered about 160 m due east of the collar of KA-7. A mafic dike transects the quartz porphyry in this vicinity, but surface alteration is not evident. Other anomalies occur near the south edge of this map but well to the southwest of the Kutam fault and shear zone, on the portion of the area surveyed using KA-1 for the downhole electrode. Of these the most conspicuous is a negative anomaly of amplitude 9 PFE aligned northeast-southwest and coincident with a zone of moderate Turam disturbances.

Plate 17 shows several strong positive anomalies not present on the previous displays. An anomaly of amplitude exceeding 15 PFE is centered about 50 m southwest of the collar of KA-3, and is possibly due to graphitic schists, which crop out in a very limited area in the immediate vicinity. However, areas of graphitic schist shown on the geologic map (pl. 3, near drill hole KA-8) have no associated IP effect. The strong negative anomaly that appears somewhat farther west of KA-3 is possibly caused by the same polarizable source.

Two positive-negative anomaly pairs, with maxima of about 10 to 12 PFE, were delineated in the region northeast of the Kutam shear zone. They are considerably offset from the ancient workings and their origin is unknown. The northwesterly of the two pairs approximately coincides with a Turam anomaly; its source may lie beneath the Wajid Sandstone, and for reasons discussed previously, should be investigated for economic potential. All of these sharply localized anomalies are in zones of low apparent resistivity for the particular electrode configuration used, as can be seen by examination of the corresponding apparent

resistivity map (pl. 19). Positive and negative IP anomalies are commonly found in mutual association when one current electrode is placed in a polarizable source that is also highly conductive. The polarized body must be both well coupled to the current source and capable of producing large charge-discharge current concentrations, although it need not coincide with the locus of such concentrations.

The maps of apparent resistivity on plates 18 and 19 are drawn at the same contour interval used for dipole-dipole pseudosections, namely, exactly 0.25 of the logarithmic exponent for resistivity values in ohm-meters. Plate 18, for drill holes KA-1 and KA-2, shows that the main area of ancient workings is a region of low apparent resistivity (electrode in KA-2). The lowest resistivity value is less than 2 ohm-meters and is located a few meters north of geodetic point D in the vicinity of KA-1. This minimum occurs about 40 m west of a resistivity low shown on dipole-dipole profile 12S (pl. 14). Similarly, a second strong minimum located south of KA-4 and detected with current electrode both in KA-1 and KA-2 is located about 40 m west of the corresponding dipole-dipole low on profile 15S. The shifts are essentially in the direction of structural dip and are probably related to the enhanced influence of deeper sources in the mise-a-la-masse method here as compared with the dipole-dipole survey, reflecting near-surface conductive zones that extend down structure. Again, the true resistivities may be quite different from the apparent values.

That the southeast end of the workings is not part of the low-resistivity anomalous zone was unexpected, for both KA-1 and KA-4 penetrated rich ore, and this area shows a substantial IP effect and is part of the principal SP anomaly. On the other hand the KA-4 minimum occurs over the Kutam fault and appears to be associated with the intense negative IP anomaly discussed above. It is totally isolated from the Turam anomaly that peaks farther southeast along the shear zone; the Turam anomaly seems to have little or no apparent resistivity expression on the mise-a-la-masse data. The latter state of affairs could well be a geometric effect and might not hold true for a different position of the remote electrode--one, say, to the south or east of the ore zone.

The several zones of anomalous IP effect in the southern part of the map area (downhole electrode in KA-1) are also zones of anomalous resistivity, but for the most part they lie outside the area of geologic mapping and have not been accounted for. Values range from more than 10,000 ohm-meters to less than 100 ohm-meters, the lowest value occurring for a spread in Wadi Kutam and therefore not necessarily attributable to bedrock.

Another surprising feature of the KA-2 map is the linear region of very high resistivity extending north to south across virtually the entire area mapped with this electrode configuration. The highest value of apparent resistivity is just under 100,000 ohm-meters. A saddle in the high resistivity ridge occurs at the collar of KA-2 and also farther north, at the northeast margin of the Kutam shear zone. In general the resistivity ridge corresponds rather closely to a topographic gradient. It is in part paralleled by magnetic trends in this vicinity, but has no IP expression. It does not appear on the KA-2 map (bottom part of pl. 18) even where the topographic gradient is still present, nor on the dipole-dipole pseudosections. A similar but laterally displaced feature appears on the apparent resistivity map of plate 19 (current electrode in KA-3). Whether the topographic break and anomaly source have a common structural control, and whether there is in fact a resistivity high beneath the anomaly, are open questions. A blind dike could produce such a linear resistivity high. In any case, the existence of a prominent resistivity barrier in this zone may have affected the results of the Turam survey because it is interposed between the ore deposit and one or more of the grounded Turam current electrodes.

Except for slight displacements of anomalies, the main features of the apparent resistivity maps for current electrodes in KA-2 (pl. 18) and KA-3 (pl. 19) are similar. Considerably more detail appears in the north on the KA-3 maps for both resistivity and IP effect, a predictable result of the contrast in proximity to the downhole electrode. Positive and negative PFE anomalies on the KA-3 map generally are roughly coincident with resistivity lows, many of which have values less than 100 ohm-meters.

The apparent-metal-conduction-factor maps of plates 20 and 21 do not reflect the linear high resistivity feature because only metal factors whose absolute value is greater than 1,000 have been contoured. The metal factors are, of course, negative where the IP effect is negative; these areas may be of some importance and therefore have been included (shading was added for contrast). For the most part the Kutam ore deposit produces high metal factor anomalies, the maximum value exceeding 100,000. However, high MF values are present in association with most of the PFE anomalies. It appears that at Kutam the metal factor is not particularly diagnostic of economic targets with mise-a-la-masse. Also the dipole-dipole pseudosections give a superior representation of metal factor contrasts.

INPUT AIRBORNE ELECTROMAGNETIC SURVEY

The INPUT^{1/} ("INDuced PULse Transient") method of airborne EM surveying is based on the transmission of powerful EM pulses from a source coil rigidly attached to the extremities of an aircraft, and the reception, as a return signal, of the transient EM secondary field generated by the flow of eddy currents induced in a subsurface conductor. The secondary field is detected by a towed sensor at the end of each transmitting pulse, and is sampled at six intervals during its decay prior to the next transmission. Penetration of up to 150-200 m is obtained because of the presence of audio-frequency components. Generally the greater the depth extent, or conductivity, or thickness of a responsive body, the slower the transient decay rate.

The INPUT system employed for the Kutam test survey was a Barringer Mark V model mounted on a PBX Super Canso aircraft, which was also equipped with a geoMetrics model G-803 proton magnetometer to record total magnetic field intensity. Lines were flown at a nominal terrain clearance of 120 m and mean spacing of 200 m. Three lines were oriented northwest and nine lines were oriented northeast, the zone of intersection being approximately over the ore deposit.

The electromagnetic map and magnetic map resulting from the INPUT survey are reproduced here on plates 22 and 23, respectively. The area covered by plates 1 to 21 on these maps is outlined by a dashed line.

Examination of plate 22 shows that most of the Kutam target area produces a conductive response, labeled by the contractor as anomalies KU-8 and KU-9. The source of KU-9 may be largely or entirely concealed beneath strata of Wajid sandstone; the source of KU-8 is apparently the Kutam ore body and associated shear zone. The intensity of the INPUT response is very weak in both cases but the decay rate is only moderate, as can be seen by the ratio of first-to-fourth channel amplitudes, and hence the contractor has classified these two anomalies as "bedrock-fair", his next-to-highest category with respect to favorability as an exploration target. In no case did the ore

¹INPUT^(R) is a registered trademark of Barringer Research, Toronto, Canada. The use of names of exploration systems and equipment in this report is for descriptive purposes only, and does not imply endorsement by the USGS Mission.

zone produce a response detected on all six channels. However, the strike extent of anomalous zone KU-8 is nearly 1.5 km, or about twice that of the known mineralized zone and three times that of the drilled ore body. The zone includes a portion of the Wajid Sandstone over which Turam and IP anomalies have been delineated. Had the flights been made at an early stage of exploration the results would have immediately pointed out the Kutam mine area as a high priority target for ground follow-up.

KU-9 is of particular interest due to its proximity to KU-8 and to the fact that the anomalous zone strikes parallel to the Kutam shear zone. The INPUT response conceivably could have been generated by a conductive hematite-cemented zone at the base of the Wajid, but it seems much more likely to be associated with high conductivity in another, parallel shear zone in Precambrian rock, and is therefore worthy of a follow-up investigation.

Several other INPUT anomalies can be seen on the map and the most prominent of these, KU-1, 3 km southwest of the Kutam mine, is also almost certainly due to a bedrock source (sulfides, hematitic iron oxides, or graphite) and deserves further investigation.

The aeromagnetic map compiled from the INPUT survey (pl. 23) shows that the Kutam mine area lies on the flank of a large positive anomaly centered about 1 km northwest of the mine. The source of this anomaly is unknown. Within the mine area the isomagnetic contours trend mostly east and gradients are very gentle (total relief is only 50 gammas (nannoteslas),

MAGNETIC SURVEY

A total-field intensity ground magnetic survey was conducted at Kutam during May 1975 by Blank, Gettings, and Merghelani, with a geoMetrics model G816 proton magnetometer (sensitivity 1 gamma). The purpose of the survey was to provide additional structural information and to aid in the interpretation of electrical and electromagnetic anomalies. Readings were taken at 20-m intervals along the east-west grid lines and also along north-south tie lines 4E, 24E, 40E, and 60E (see base map, pl. 1). After line adjustments and correction for temporal drift by comparison with near-continuous base station readings, the absolute field intensity values--except where gradients are steep--are probably accurate to within several gammas. The reduced data have been contoured at intervals of 5, 10, and 50 gammas to produce the total-magnetic field intensity anomaly map of plate 24. No regional gradient has been removed but the datum has been lowered

by 38,000 gammas. The parameters of the earth's main field (International Geomagnetic Reference Field (IGRF) Epoch 1965.0 extrapolated to 1975.5) are: declination 0.51°E. , inclination 23.48° , total intensity 39058 gammas.

The anomaly map shows a weak decrease in intensity levels from north to south (this gradient is much stronger than the IGRF gradient; compare aeromagnetic map of plate 23) and a concentration of high-amplitude anomalies south of the ancient mine workings. The southern part of the map area is also characterized by strong east-west trends. The latter features are not a consequence of traverse orientations but instead are believed to belong to the set of regional east-west anomalies commonly seen on small-scale aeromagnetic maps of the southern Arabian Shield. In some cases the regional anomalies are clearly associated with late Precambrian (Najd or post-Najd?) shear zones, which may or may not be revealed by mappable offsets of formations. Unfortunately, however, the Kutam ancient mine lies just outside the area of regional aeromagnetic coverage and a direct comparison with the regional maps cannot be made.

The east-west magnetic trends at Kutam occur in a belt of parallel SP and IP trends. None of these anomalies has yet been satisfactorily explained, and no east-west structural elements have yet been identified in this vicinity. Nevertheless the coincidence of magnetic, SP, and IP trends with a set of regional east-west shear trends may be significant from the standpoint of exploration in the southern shield, because it tends to confirm the existence of such structures in the Kutam area, and the east-west IP anomaly appears to mark the southern boundary of the ore body (see discussion of IP results). Thus an east-west shear may have provided an important control for ore deposition or else produced an offset of the ore body, depending on the relative ages of faulting and mineralization. This hypothesis might be worth further investigation. A more extensive discussion of the significance of geophysical trends is given in the concluding section of the report.

A zone of weak intensity contrasts, that is, a magnetically "quiet" zone, occurs over the ancient mine workings and in a zone of intense pyritization and oxidation extending northwest from the vicinity of survey point D over the Kutam ore body. Both the highly sheared sericite-chlorite schist unit that constitutes the host rock for mineralization and the adjacent silicified quartz porphyry appear to have an abnormally weak magnetic expression, possibly as a result of leaching of magnetite during shearing and hydrothermal alteration. Relatively unaltered quartz

porphyry outside the principal shear zone in some places shows strong magnetic contrasts and in others has little expression.

The quiet zone associated with the altered area is sharply bounded on the southwest by two linear negative anomalies whose axes lie roughly along the Kutam fault. The lows and related trends are discontinuous in the vicinity of drill hole KA-2; southeast of here the Kutam fault has no marked magnetic expression. However, a similar anomaly pattern continues southward, passing east of the collar of KA-5. Anomaly patterns west of KA-5 also suggest a change in structural grain from southeasterly to southerly. In fact the western margin of a belt of low contrast may trend toward the south, or even slightly southwesterly, between KA-4 and KA-8 (the trend of the eastern margin might be considered southwesterly). In general, magnetic trends in the southern half of the map area show more influence of north-south structures than do trends in the northern half, although in no case has the source of any magnetic anomaly been specifically identified.

The strongest discrete anomalies occur to the east and west of drill hole KA-8 and are probably associated with diabase dikes or small bodies of gabbro, tectonically juxtaposed with or intruded by quartz porphyry; in the southeast corner of the map these are roughly coincident with Turam anomalies. Most lie just outside the area of detailed geologic mapping. Areas of mapped amphibolite-grade metasedimentary and metavolcanic rocks in general lack strong magnetic contrasts. Several small anomalies appear to be directly associated with the collars of drill holes KA-1, KA-2, KA-3, and KA-5, perhaps due to proximity of casing and capping steel to points of observation. The most intense anomaly on the map is centered on drill hole KA-6 and can be attributed to the presence of a drilling rig and drill stems in this vicinity at the time of the survey.

SUMMARY AND CONCLUSIONS

The most prominent geophysical anomalies detected by the various ground surveys in the vicinity of the Kutam ancient mine have been brought together on the combined anomaly map of plate 25. This map shows areas of anomalous radiometric activity (gamma-ray events above the K^{40} energy threshold, greater than 100 cps), negative self-potential (greater than 75 mv negative with respect to geodetic station B), Turam electromagnetic response (reduced amplitude ratio greater than 110 percent, 660 Hz), and induced polarization (PFE greater than 5 for mise-a-la-masse surveys with downhole electrode in KA-1, KA-2,

and KA-3). Also shown are approximate maximum widths of sources for dipole-dipole profile anomalies in IP effect (PFE greater than 4) and apparent resistivity (ρ_a less than 100 ohm-meters at 0.3 Hz).

Selection of anomaly thresholds for the combined plot has of course been arbitrary. To avoid undue confusion, anomalies in certain of the Turam and IP parameters are not included; no negative IP anomalies are shown, and magnetic results are omitted entirely. Surface projections of sources and anomalies in the dipole-dipole pseudosections are crude at best. Finally, the area of coverage is not always the same in different surveys, and hence the anomaly distributions can be deceptive.

Nevertheless it is clear that the drilled Kutam ore deposit is approximately outlined by the area common to self-potential and induced polarization anomalies, which has a maximum strike length of about 400 m and a maximum width less than 100 m; and that the principal SP, Turam, and IP anomalies together outline the Kutam shear zone, producing a pattern with an overall trend of about N.45°W. but with a more northerly internal an echelon fabric, which could reflect the influence of oblique structures. That the ore deposit is essentially an SP-IP target, rather than an EM induction target, is perhaps the most important conclusion of the geophysical investigations.

The lack of a strong Turam EM response over the known ore can be attributed in part to the method of survey, but it is likely that the deposit is at best only weakly conductive, a condition possibly related to the spatial coincidence of mineralization and silicification and also to prevalence of essentially a one-dimensional, steeply plunging structural habit of the ore. Although the deposit may have numerous internal electrical short-circuits, the total area coupled to an electromagnetic inducing field is probably not very large compared with that of a sheet-like conductor of the same strike extent and ore content.

Strong Turam anomalies northwest and southeast of the ore deposit are not associated with mapped or logged mineralization or anomalous IP effects, but they are disposed in low-lying zones of shallow conductive and pyritically altered rock in the Kutam shear zone. They are interpreted as the effect of galvanic current concentrations in near-surface ionic conductors in weakly mineralized wet shears.

Zoning of mineralization and alteration along the Kutam shear structure may be the fundamental factor accounting for the geophysical responses observed. The zone of silicification

associated with copper mineralization is relatively resistant to erosion, in contrast to zones of pyritic alteration that flank the ore deposit in either direction. Therefore the ore zone crops out at relatively high elevation (the ancient diggings are predominantly on the crest of a ridge). Depth to water table, as determined by electric logs of KA-1, KA-2, KA-3, and KA-4 (pl. 6), increases markedly with topographic elevations, ranging from about 20 to 40 m. This relatively greater depth to water table in the mineralized zone could account for the weak Turam response over the deposit even if this response, like that of the pyrite zones, was ionic. Moreover there is also relatively less pyrite in the ore zone, and a lower pyrite content may be associated with lower electrical conductivity of the ionic solutions.

Many anomalies are seen on plate 25 that appear to have no relation to the Kutam shear zone. To what extent can they be used as guides for mineral exploration? Unfortunately their origins remain quite unexplained, but none of them appears to have economic potential comparable to that of the shear zone. Overlapping Turam and IP anomalies where basement rock is concealed beneath Wajid sandstone, north of the Kutam shear zone but on strike with north-trending mineralization, are recognized as one possible exploration target. Coincident SP and IP anomalies (both dipole-dipole and mise-a-la-masse) in the southwest corner of the area of coverage are perhaps another, even though the geochemical survey showed no anomalous copper or zinc in this area. Dipole-dipole pseudosections suggest that the polarizable source associated with the Kutam ancient mine has deepened and moved laterally to the west between lines 15S and 18S. Additional dipole-dipole lines, using longer dipoles, might show continuity of the IP anomaly of line 15S with that of line 21S or might show clearly a fault offset, in which case the southern area would hold considerable promise. The PFE results from line 15S most likely reflect mineralization in the shear zone adjacent to the Kutam fault, as encountered in KA-4; the negative IP anomaly system in the mineralized area extends south and west from here, and perhaps so does the mineralization. Drill hole KA-8, which investigated the southeastern Turam anomaly, would probably have completely missed any deep mineralization offset southwesterly.

A modicum of support for westward displacement of ore at depth is found in the magnetic data. The zone of sheared and altered quartz porphyry and chlorite-sericite schist that contains chalcopyrite and pyrite mineralization at Kutam shows up on the magnetic map as a relatively quiet zone lacking

strong magnetic contrasts, particularly where the alteration has been most intense--magnetite appears to have been leached from at least the upper portion of the zone of mineralization. It may be significant that this quiet zone appears to curve somewhat to the southwest at its southeastern end.

Trends of the various geophysical anomalies are assembled on the map of plate 26. This map depicts "strong" and "weak" axial and gradient trends of magnetic total-field intensity, SP, Turam reduced-amplitude ratio (660 Hz), and IP mise-a-la-masse apparent resistivity and PFE anomalies (as well as dipole-dipole anomalies). Subjective though the representation of these trends may be, their overall pattern lends itself to a number of observations having to do with structural interpretation, as follows:

1) The Kutam shear zone structural trend (N.45°W.) is easily predominant in the north half of the map, which includes the drilled ore body and the most intense zone of pyritic alteration. N.20°W. trends, or intermediate directions between north and northwest, are subordinate.

2) The continuity of the Kutam trend set as a concentrated belt is clearly interrupted at the southeastern end of the ancient workings. From here on to the south the S.45°E. trends, although present, are no more conspicuous than those of easterly and northeasterly orientations. Evidently this southern zone is one of considerable structural complexity.

3) Kutam trends tend to bend to the south or southwest in the southernmost part of the map area, many trend lines are convex eastward, and northeasterly trends become important. These trends suggest folding or the influence of a conjugate set of shears.

4) A well-defined belt of east-west trends appears immediately to the south of the ancient workings. It has a width of about 250 m, and is parallel to many regional magnetic features in the southern shield, most of which have little or no geologically mapped expression. (An east-west fault that cuts Wajid sandstone was mapped by Anderson (1978) about 1.5 km south of the Kutam prospect.) The east-west belt of Kutam may represent a late Precambrian shear zone of unknown offset. The fact that it is spatially related to the southeastern termination of the known Kutam ore deposit suggests that it may have exerted a controlling influence on ore localization or been responsible for a right lateral offset of the deposit.

5) A belt of northwest trends is present in the southwest corner of the map area, south of the belt of east-west trends. This belt may reflect the boundary of a mineralized shear zone parallel to the Kutam system.

6) The strong north-south IP trend across the western part of the map is suspiciously continuous and linear. Other north-south trends do exist; for example, the Turam trends across the north-central part of the map, but they do not coincide with the IP trend and are less conspicuous. Little or no geologic evidence of such a structural orientation exists here, and it is difficult to conceive of the IP trend as due to a simple high-resistivity feature such as a fault or a buried dike, in the absence of supporting surface data. The very intense apparent resistivity ridge may in some way be an artifact of the survey or data reduction process.

7) The most significant deduction from anomaly trends may relate to the apparent en echelon disposition of the three major anomalies (northwestern Turam, central IP/SP, and southeastern Turam) in the Kutam shear zone. (This disposition is somewhat masked on plate 26 by the abundance of lesser trends.) Three possible explanations are suggested. None addresses the possibility of a westerly extension of the Kutam ore zone at depth, south of the ancient workings (in the belt of east-west trends), which would require either a change in dominant ore controls in that area from the Kutam shear zone to a favorable lithologic zone or fold structure, or a subsequent tectonic offset of the mineralized shear zone. They are: 1) The primary structural control of mineralization at Kutam was a set of en echelon tension fractures resulting from right-lateral movement in the Kutam shear zone. Mineralization according to this interpretation would be largely or entirely post-shearing. 2) The primary control of mineralization was simply the intersection of the Kutam shear zone with a set of north-trending structures, which produced a permeable environment suitable for ore deposition. Subsequent shearing has shifted the pyritized hanging wall to the northwest, and the less pyritized footwall to the southeast, relative to the bulk of the ore body. This hypothesis requires mineralization to have been contemporaneous with shearing. 3) The en echelon disposition of the anomalies is more apparent than real, or if real it has no geologic significance other than to reflect the influence of north-trending structures on geophysical response. The geophysical work does not offer any means of discriminating among these three hypotheses.

Although it has been suggested in this report that specific areas southwest and north of the Kutam mine should be prospected, the best chance for extending ore reserves at Kutam may be to explore at depth beneath the Turam anomalies in the principal shear zone. If the pyrite/chalcopyrite relation is zoned vertically as well as laterally, then the pyrite associated with those anomalies could become enriched at depth by increasing admixtures of zinc and copper sulfide. There is almost no chance that a very deep base metal concentration could have been detected at the depths of exploration reached by the ground surveys. The INPUT data imply that conductivity in the southeastern corner of the map area dies off less rapidly with depth than that in the immediate vicinity of the mine. Sulfide mineralization is known from Noranda drilling results to plunge 40° to 60° southeasterly, and to date the only proved mineralization in the area is associated with the Kutam shear zone. This zone might offer a reasonable target for pulsed EM probes with a large depth penetration capability.

REFERENCES CITED

- Anderson, R. E., 1978, Geology of the Mayza quadrangle, sheet 17/43 B, Kingdom of Saudi Arabia: Saudi Arabian Directorate General of Mineral Resources Geological Map GM-31, scale 1:100,000.
- Anonymous, 1978, Airborne electromagnetic survey, Barringer "INPUT" system, Shuwas, Bidah, Kutam test, Kamal, Khnaiguiyah, Al Amar North, Gith Gath, and Masane areas, Kingdom of Saudi Arabia: Arabian Geophysical and Surveying Co. (ARGAS), Final Report, Geoterrex Ltd., 1977 INPUT survey, 2 parts, 383 p., 34 electromagnetic plan maps and 34 aeromagnetic contour maps, scale 1:20,000.
- Corwin, R. F., and Hoover, D. B., 1979, The self-potential method in geothermal exploration: Geophysics, v. 44, no. 2, p. 226-245.
- Heiland, C. A., 1940, Geophysical Exploration: Prentice-Hall, N.Y., 1013 p.
- Keller, G. V., and Frischknecht, F. C., 1966, Electrical Methods in Geophysical Prospecting: International Series of Monographs on Electromagnetic Waves, v. 10, Pergamon Press, N.Y., 513 p.
- Smith, C. W., Anderson, Ernest, and Dehlavi, M. R., 1978, Geology and ore deposits of the Kutam mines, Kingdom of Saudi Arabia: U.S. Geological Survey open-file report 78-519, (IR)SA-211.

Sumner, J. S., 1976, Principles of induced polarization for geophysical exploration: Developments in Economic Geology, 5, Elsevier Science Publishing Company, Amsterdam, 277 p.

Telford, W. M., Geldart, L. P., Sheriff, R. E., and Keys, D. A., 1976, Applied Geophysics: Cambridge University Press, Cambridge, 860 p.

Wynn, J. C., and Blank, R. H., 1979, A preliminary assessment of the 1977 input survey on the Arabian Shield, Kingdom of Saudi Arabia, with guides for interpretation and ground follow-up: U.S. Geological Survey open-file rept. 79-1508, (IR)SA-268.

APPENDIX

Appendix 1.--*Reduction of Turam data obtained at 20-m receiver spacing to ratio and phase anomalies at 40-m spacing.*

In the ABEM manual (ABEM Instrument Group, Leaflet MR 5280 E) provided with the equipment used for the Kutam surveys, it is specified that reduced amplitude ratios must be squared and phase differences must be doubled when the distance between receivers is halved with respect to the standard distance, so that all values to be plotted are appropriate for the standard distance. This procedure distorts the data somewhat and is therefore less satisfactory than making an exact transformation, which was done in converting the Merghelani and Flanigan data of March 1974, obtained at 20-m receiver spacing, to data at 40-m spacing, for comparison with the results of the Merghelani and Blank survey of November 1974. The latter procedure is as follows: multiply the reduced ratio values for adjacent plot points to get a new reduced ratio for a plot point midway between the previous two, and for twice the spacing; algebraically add adjacent phase differences to get the new phase difference at the mid-point for twice the spacing.

The rationale for this procedure is as follows:

Let $R_f|_N$ = measured amplitude ratio for position N, with receivers at positions N-1 and N+1.

$R_n|_N$ = normal amplitude ratio for position N, with receivers at positions N-1 and N+1.

$R_d|_N$ = reduced amplitude ratio for position N, with receivers at positions N-1 and N+1.

$A_f|_N$ = actual field amplitude at position N.

$A_n|_N$ = normal field amplitude at position N.

Then by definition,

$$R_d \Big|_N = \frac{R_f \Big|_N}{R_n \Big|_N} = \frac{A_f \Big|_{N-1} / A_f \Big|_{N+1}}{A_n \Big|_{N-1} / A_n \Big|_{N+1}}$$

Similarly

$$R_d \Big|_{N+2} = \frac{A_f \Big|_{N+1} / A_f \Big|_{N+3}}{A_n \Big|_{N+1} / A_n \Big|_{N+3}}$$

$$\begin{aligned} \therefore R_d \Big|_N \cdot R_d \Big|_{N+2} &= \frac{A_f \Big|_{N-1} / A_f \Big|_{N+1}}{A_n \Big|_{N-1} / A_n \Big|_{N+1}} \cdot \frac{A_f \Big|_{N+1} / A_f \Big|_{N+3}}{A_n \Big|_{N+1} / A_n \Big|_{N+3}} \\ &= \frac{A_f \Big|_{N-1} / A_f \Big|_{N+3}}{A_n \Big|_{N-1} / A_n \Big|_{N+3}} \\ &= R_d \Big|_{N+1} \end{aligned}$$

, for receivers at positions
N-1 and N+3, that is, at
twice the previous spacing.

Also it is evident that

$$\Delta \phi \Big|_{N-1, N+3} = \Delta \phi \Big|_{N-1, N+1} + \Delta \phi \Big|_{N+1, N+3}$$

where the $\Delta \phi$'s are the phase differences between the points indicated.